Analytical and Bioanalytical Chemistry
https://doi.org/10.1007/s00216-020-02831-1

REVIEW

2D materials in electrochemical sensors for in vitro or in vivo use

Raluca-Elena Munteanu[1] · Paola Sánchez Moreno[2] · Mattia Bramini[2,3] · Szilveszter Gáspár[1]

Received: 28 May 2020 / Revised: 15 July 2020 / Accepted: 17 July 2020

Abstract

Individual cells and cell populations are at the present time investigated with a myriad of analytical tools. While most of them are commercially available, some of these analytical tools are just emerging from research laboratories and are in the developmental phase. Electrochemical sensors which allow the monitoring of low molecular weight compounds released (and / or uptaken) by cells are among these emerging tools. Such sensors are increasingly built using 2D materials (e.g. graphene-based materials, transition metal dichalcogenides, etc.) with the aim of conferring better analytical performances to these devices. The present work critically reviews studies published during the last 10 years describing electrochemical sensors made with 2D materials and exploited to monitor small compounds (e.g. H_2O_2, ·NO, glucose, etc.) in living biological systems. It also discusses the very few 2D material-based electrochemical sensors which are wearable or usable in vivo. Finally, the present work includes a specific section about 2D material biocompatibility, a fundamental requirement for 2D material-based sensor applications in vitro and in vivo. As such, the review provides a critical view on the state of the art of electrochemical sensors made with 2D materials and used at cellular level and it evaluates the possibility that such sensors will be used on / in the human body on a wider scale.

Keywords Electrochemical sensors · 2D materials · Living cells · Biocompatibility

Introduction

In vitro cell cultures are currently studied in order to reveal the biochemical and molecular background of different disorders or to predict the effect on humans, animals or plants of a drug candidate, a new material, or an environmental pollutant. Experiments, at both individual cell level and cell population level, are facilitated by a myriad of analytical tools developed to monitor different cellular parameters (e.g. light and electron microscopy, spectrophotometry, electrophoresis, etc.). Among these analytical tools one finds also electrochemical sensors. Such sensors are currently mainly used to monitor small molecular weight compounds which are either released or uptaken by cells. For example, carbon fiber microelectrodes have been used to monitor the release of catecholamine neurotransmitters both in vivo and in vitro. These microelectrodes facilitated the discovery of several important details of neurotransmission [1]. Although very few electrochemical sensors for the investigation of living cells are commercially available, they have at least four important advantages as compared to most standard analytical tools. First, electrochemical sensors detect the analyte of interest without the need of loading the cells with reagents (while optical methods most often need the cells to be loaded with fluorescent dyes). This is advantageous as loading the cells with reagents can sometimes change the properties of the investigated cells (e.g. the mechanical properties [2]). Second, electrochemical sensors are relatively easily fabricated in different sizes and thus facilitate analyzing samples ranging from single cell to millions of cells and explanted tissues. Moreover, electrochemical sensors have been already miniaturized to the point where they can also be used in the intracellular space of one single cell [3]. Third, electrochemical sensors are reversible in the sense that they can monitor both the production and the subsequent consumption of the analyte of interest. This is advantageous compared to assays in which the optical properties of the used fluorescent dyes change irreversibly in the presence of the targeted analyte. Forth, electrochemical sensors usually have

Published in the topical collection *2D Nanomaterials for Electroanalysis* with guest editor Sabine Szunerits.

✉ Szilveszter Gáspár
sgaspar@biodyn.ro

[1] International Centre of Biodynamics, 1B Intrarea Portocalelor, 060101 Bucharest, Romania

[2] Department of Applied Physics, Faculty of Sciences, University of Granada, Avenida Fuente Nueva S.N., 18071 Granada, Spain

[3] Center for Synaptic Neuroscience and Technology, Istituto Italiano di Tecnologia, L.go Rosanna Benzi 10, 16132 Genoa, Italy

Published online: 10 August 2020

short response times (from ms to s) and this makes the observation of the production or consumption dynamics of the analyte of interest easier (instead of reporting only endpoints). The time evolution of a cellular parameter can reveal additional details about the way cells interact with the test compound.

In order to improve the analytical performances of electrochemical sensors, a variety of electrode materials (e.g. Au, Pt, glassy carbon, carbon fiber, etc.) were combined with an even larger variety of nanomaterials during the years [4]. In this context, the discovery of graphene in 2004 [5], as well as the consequent research on non-graphene 2D materials, had a powerful impact on the field of electrochemical sensing as pointed out in several review articles [6–11]. It was rapidly discovered that 2D materials could improve the analytical performances of electrochemical sensors by increasing their electrochemically active surface area and electrical conductivity and /or by providing new ways of interacting with the targeted analyte (e.g. π-π interactions). Taking into account all these aspects, the present review focuses on 2D material-based electrochemical sensors used to investigate living cells and tries to summarize the last 10 years of research in the field. The review will firstly present electrochemical sensors made with graphene-based materials (GBMs) (Section 2), secondly electrochemical sensors made with non-graphene 2D materials (Section 3) and then electrochemical sensors made with 2D materials which are wearable or suitable for in vivo use (Section 4). The biocompatibility of 2D materials will also be discussed (Section 5) before drawing conclusions (Section 6).

Electrochemical sensors built with graphene-based materials

The 2D materials most often used to enhance the performances of electrochemical sensors are those based on graphene (i.e. graphene, graphene oxide, GO, reduced graphene oxide, rGO, etc.). However, in spite of the initial enthusiasm surrounding the use of GBMs as electrocatalysts, these materials turned out to be rather poor electrocatalyst [12]. Therefore, it is not a surprise that most electrochemical sensors built with GBMs are also relying on either doping (e.g. with N and S [13] or with N and B [14]) or additional electrocatalysts (see Table 1). The GBMs still provide benefits such as good electrical conductivity, increased electrochemically active surface area, and better dispersion of the catalysts [20, 23–25, 44]. Figure 1 shows the main steps of making an electrochemical sensor that is based on rGO, hemin and Au nanoparticles, and that is used for the detection of H_2O_2 released from HeLa cancer cells (see inset). Similar sequences of steps are used to build most of the electrochemical sensors made with GBMs.

The analytical performances of the sensor schematically presented in Fig. 1 are listed in Table 1 together with details about other electrochemical sensors made with GBMs and used to investigate living cells.

To gain a better grasp on the electrochemical sensors made with GBMs and used to investigate living cells, let us analyze the content of Table 1 column by column.

As one can observe in the first column of Table 1, about 71% of the electrochemical sensors made with GBMs and used to investigate living cells were developed for the detection of H_2O_2. This molecule is an important signaling molecule in eukaryotes but it can also cause oxidative stress if overproduced [55]. Of note, oxidative stress is among the major causes of several disorders, such as cardiovascular [56] and neurodegenerative diseases (e.g. Parkinson's disease [57] and Alzheimer's disease [58]), atherosclerosis [59] and cancer [60]. About 19% of the electrochemical sensors made with GBMs were developed for the detection of ·NO. This molecule, just as H_2O_2, plays an important role both in physiological conditions (e.g. in vascular muscle relaxation [61]) and in pathological circumstances (e.g. in cancer [62], arthritis [63], autoimmune diseases [63], etc.). While H_2O_2 is most often detected by setting the electrochemical sensor to negative potentials (up to −750 mV vs. Ag/AgCl), ·NO is most often detected by setting the electrochemical sensor to positive potentials (up to +840 mV vs. Ag/AgCl). In addition to H_2O_2 and ·NO, the evolution of the concentration of $O_2^{\cdot -}$ [44], NO_2^- [16], H^+ ions (i.e. pH) [47], or glutamate [53] in the extracellular space of living cells was also investigated using electrochemical sensors made with GBMs. Constant potential amperometry was most often the electrochemical method of choice when using the sensors at cellular level. This electrochemical method is characterized by simplicity, high temporal resolution (down to ms), and advantageously low contribution from capacitive currents.

Relatively large (e.g. 3 mm in diameter) glassy carbon electrodes were used to develop 29 out of the 42 electrochemical sensors listed in Table 1. The popularity of these electrodes is not surprising because glassy carbon electrodes not only have good electrochemical properties but are also significantly cheaper than other traditional electrodes (e.g. those made of Au or Pt). On the contrary, what is somewhat surprising is that the reviewed literature reveals no tendency to miniaturize the graphene-based electrochemical sensors to investigate living cells. Although micrometer-sized devices can facilitate single cell observations, only 4 out of the 42 electrochemical sensors listed in Table 1 were built using electrodes miniaturized to some degree (e.g. carbon fiber microelectrodes [47]). ITO was also used a couple of times as base electrode. This electrode material is very interesting as its transparency allows combining the electrochemical detection with the optical observation of the investigated cells. However, this possibility was not yet explored.

Table 1 Electrochemical sensors made with GBMs and used to investigate living cells (Observations: Sensors are listed in chronological order. DL, LR, S, and RT stay for detection limit, linear range, sensitivity, and response time, respectively)

Analyte / Applied potential	Sensor structure	Analytical performances	Investigated cells / Stimulus	Ref.
H_2O_2 / -150 mV vs. Ag/AgCl	"Paper" made of rGO modified with MnO_2 nanowires and Pt nanoparticles	DL = 1 μM; LR = 2 μM - 13 mM; S = 129.5 μA mM^{-1} cm^{-2}; RT = 3 s	(Human) HepG2 / N-formyl-L-methionyl-L-leucyl-phenylalanine (fMLP)	[15]
NO_2^- / +750 mV vs. saturated calomel electrode (SCE)	Glassy carbon modified with graphene that was modified with potassium	DL = 0.2 μM; LR = 0.5 μM – 7.8 mM; RT = 2 s	(Human) HL-60 and SMMC-7721 / Lipopolysaccharide	[16]
H_2O_2 / -270 mV vs. Ag/AgCl, KCl (sat)	Glassy carbon modified with rGO and CuS nanoparticles	DL = 0.3 μM; LR = 5 μM – 1.5 mM; S = 0.035 μA $μM^{-1}$; RT = 2 s	(Human) HeLa / CdTe quantum dots	[17]
H_2O_2 / -250 mV vs. SCE	Glassy carbon modified with N and B co-doped graphene	DL = 0.05 μM; LR = 0.5 μM – 7.5 mM; RT = 2 s	(Human) CCRF-CEM / fMLP	[14]
H_2O_2 / -250 mV vs. Ag/AgCl, KCl (sat)	Glass slide modified with a 3D graphene foam further modified with poly(dopamine) and thionine	DL = 80 nM; LR = 0.4–660 μM; S = 169.7 μA mM^{-1}; RT = 3 s	(Human) MD-435 / fMLP	[18]
·NO / +800 mV vs. Ag/AgCl	Glassy carbon modified with rGO and Au nanoparticles	DL = 133 nM; LR = up to 3.38 μM; S = 5.38 μA $μM^{-1}$ cm^{-2}; RT = 3 s	(Human) HUVEC / Acetylcholine	[19]
H_2O_2 / -80 mV vs. Ag/AgCl	Glassy carbon modified with rGO and then with Pt nanoparticles	DL = 0.2 μM; LR = 5 μM – 3.5 mM; S = 459 mA M^{-1} cm^{-2}; RT = 5 s	(Rat) PC12 / Ascorbic acid	[20]
H_2O_2 / -300 mV vs. SCE	Glassy carbon modified with rGO modified with Fe_3O_4	DL = 0.17 μM; LR = 1 μM – 20 mM; S = 387.6 μA mM^{-1} cm^{-2}	(Human) HeLa cells/ CdTe quantum dots	[21]
H_2O_2 / -750 mV vs. Ag/AgCl	Glassy carbon modified with rGO modified with mesoporous silica and Au nanoparticles	DL = 60 nM; LR = 0.5 μM – 50 mM; S = 39.2 μA mM^{-1} cm^{-2}; RT = 2 s	(Human) HeLa and HepG2 / Phorbol 12-myristate 13-acetate (PMA)	[22]
·NO / +800 mV vs. SCE	Glassy carbon modified with rGO and CeO_2 hexagonal nanocrystals	DL = 9.6 nM; LR = 18.0 nM - 5.6 mM; S = 1676.06 mA cm^{-2} M^{-1}	(Human) A549 / Acetylcholine	[23]
·NO / +810 mV vs. Ag/AgCl	Glassy carbon modified with 3D reduced graphene hydrogel and Au nanoparticles	DL = 9 nM; LR = 0.2–6 μM; S = 45 nA $μM^{-1}$; RT = 3 s	(Mouse) JB6-C30 and B16-F10 / Acetylcholine	[24]
H_2O_2 / -100 mV vs. Ag/AgCl, KCl (sat)	Glassy carbon modified with porous rGO and Pt nanoparticles	DL = 0.5 μM; LR = 1 μM – 1.5 mM; S = 341 μA mM^{-1} cm^{-2}; RT = 3 s	(Human) HeLa / CdTe quantum dots	[25]
·NO / +750 mV vs. Ag/AgCl	Indium tin oxide (ITO) modified with rGO, a metalloporphyrin and 3-aminophenylboronic acid	DL = 55 pM; S = 37.6 μA $μM^{-1}$ cm^{-2}; RT = 400 ms	(Human) HUVEC / L-Arginine	[26]
H_2O_2 / -50 mV vs. Ag/AgCl	Paper made of graphene modified with Pt nanoparticles and carbon nanotubes	DL = 10 nM; LR = up to 25 μM; S = 1.41 μA M^{-1} cm^{-2}; RT = 3 s	Macrophage / PMA	[27]
H_2O_2 / 0 mV vs. SCE	Glassy carbon modified with reduced graphene sheets and Pt-Au bimetallic nanoparticles	DL = 0.31 μM; LR1 = 1 μM – 1.78 mM; S1 = 7.35 μA M^{-1}; LR2 = 1.78–16.8 mM; S2 = 1.13 μA M^{-1}	(Rat) PC12 / Lipopolysaccharide	[28]
H_2O_2 / 0 mV vs. Ag/AgCl	Glassy carbon modified with rGO decorated with Au, Fe_3O_4 and Pt nanoparticles	DL = 0.1 μM; LR = 0.5 μM – 11.5 mM; RT = 4 s	(Human) HeLa, U87 and HepG2 / Ascorbic acid	[29]
H_2O_2 / -400 mV vs. SCE	Carbon fiber modified with rGO modified with MnO_2 and Au	DL = 2 μM; LR = 50 μM – 14.2 mM; S = 0.167 mA mM^{-1} cm^{-2}	(Human) HeLa and HBL-100 / fMLP	[30]
H_2O_2 / -400 mV vs. SCE	Glassy carbon modified with chitosan, GO, poly (diallyldimethylammonium chloride), Au nanoparticles and horseradish peroxidase (HRP)	DL = 7.5 nM; LR = 0.0198–1.04 μM; S = 0.55 A M^{-1}; RT = 4 s	(Human) primary neutrophils and K562 / Ascorbic acid	[31]
·NO / +840 mV vs. Ag/AgCl, KCl (3 M)	Glassy carbon modified with rGO and AuPt nanoparticles	DL = 2.88 nM; LR1 = 0.02–0.4 μM; S1 = 7.35 μA M^{-1}; LR2 = 0.4–50 μM; S2 = 1.13 μA M^{-1}; RT = 4 s	(Rat) H9C2 / L-Arginine	[32]
H_2O_2 / -50 mV vs. SCE	Au modified first with rGO (that carries chitosan and ferrocene carboxylic acid) and then with Pt nanoparticles	DL = 20 nM; LR = 0.02–3 μM; RT = 2 s	(Human) HepG2, LO2 and A549 / Ascorbic acid	[33]
H_2O_2 / 0 mV vs. Ag/AgCl	Glassy carbon modified with a nanocomposite made of CuI and graphene	DL = 0.2 μM; LR1 = 0.5–25 μM; S1 = 424.4 μA mM^{-1} cm^{-2}; LR2 = 25 μM – 3 mM; S2 = 273.04 μA mM^{-1} cm^{-2}	(Human) HeLa, HepG2 and U-87 MG / Ascorbic acid	[34]

Table 1 (continued)

Analyte / Applied potential	Sensor structure	Analytical performances	Investigated cells / Stimulus	Ref.
·NO / -600 mV vs. Ag/AgCl	Pt modified with N-doped graphene nanosheets functionalized with porphyrin	DL = 1 nM; LR = 10 nM – 10 μM; S = 3.62 μA μM^{-1}	(Mouse) RAW 264.7 / Lipopolysaccharide	[35]
H_2O_2 / -450 mV vs. Ag/AgCl	Glassy carbon modified with rGO modified with methylene blue	DL = 60 nM; LR = 0.5 μM – 11.68 mM; S = 10.2 μA mM^{-1} cm^{-2}; RT = 2 s	(Human) Hep3B, HepG2, HeLa, and HEK 293 / PMA	[36]
H_2O_2 / -600 mV vs. Ag/AgCl, KCl (sat)	Paper made of graphene framework modified with 3D ionic liquid and Au nanoflowers	DL = 100 nM; LR = 0.5 μM – 2.3 mM; S = 425.6 μA M^{-1} cm^{-2}; RT = 3 s	(Human) HBL-100, MDA-MB-231 and MCF-7 / PMA	[37]
H_2O_2 / -400 mV vs. Ag/AgCl	Glassy carbon modified with 3D P-doped graphene	DL = 0.17 μM; LR = 0.2 μM – 41.2 mM; RT = 2 s	(Human) HeLa / fMLP	[38]
H_2O_2 / -700 mV vs. SCE	Glassy carbon modified with porous graphene and HRP	DL = 0.0267 nM; LR1 = 0.08 nM-0.664 μM; LR2 = 2.77 μM – 0.83 mM; S2 = 5.2 nA μM^{-1}	(Rat) PC12 / Ascorbic acid	[39]
H_2O_2 / -500 mV vs. SCE	Glassy carbon modified with graphene and N and S co-doped graphene quantum dots	DL = 26 nM; LR = 0.4 μM – 33 mM; RT = 3 s	(Mouse) RAW 264.7 / CdTe quantum dots	[13]
H_2O_2 / - 200 mV vs. Ag/AgCl	Glassy carbon modified with rGO carrying PtPb nanoplates	DL = 2 nM; LR = 2 nM – 2.5 mM; S = 4.05 mA mM^{-1} cm^{-2}	(Mouse) RAW 264.7 / fMLP	[40]
H_2O_2 / -600 mV vs. Ag/AgCl	Glassy carbon modified with rGO modified with PtNi nanowires	DL = 0.3 nM; LR1 = 1–223 nM; LR2 = 363 nM – 5.3 mM	(Mouse) RAW 264.7 / fMLP	[41]
H_2O_2 / -200 mV vs. Ag/AgCl	Glassy carbon modified with GO modified with Fe_3O_4 quantum dots	DL = 78 nM; LR = 0.8–334.4 μM; S = 274.15 mA M^{-1} cm^{-2}; RT = 2.8 s	(Human) A549 / PMA	[42]
H_2O_2 / -100 mV vs. SCE	Glassy carbon modified with graphene nanosheets carrying SnO_2 and Pd-Pt nanocages	DL = 0.3 μM; LR = 1–300 μM; S = 0.240 μA μM^{-1}; RT = 3 s	(Human) HeLa cells / Ascorbic acid	[43]
$O_2^{\cdot -}$ / 500 mV vs. SCE	Glassy carbon modified with electrospun fibers containing amorphous carbon, rGO, and $FePO_4$	DL = 9.7 nM; LR = 10 nM – 10 μM; S = 9.6 μA M^{-1} cm^{-2}; RT = 1.6 s	(Human) HeLa / Zymosan	[44]
·NO / +900 mV vs. SCE	ITO modified with iron phtalocyanine-functionalized, N-doped graphene	DL = 180 nM; LR = 0.18 μM- 0.4 mM; S = 0.21 μA μM^{-1} cm^{-2}; RT ~ 4 s	(Human) HUVEC / L- Arginine	[45]
H_2O_2 / -400 mV vs. Ag/AgCl, KCl (sat)	Glassy carbon modified with rGO carrying trimetallic Au-Pt-Pd nanoparticles	DL = 2 nM; LR = 0.5 μM – 1 mM; S = 278 mA M^{-1} cm^{-2}; RT = 3 s	(Human) MDA-MB-231 and T47D / Ascorbic acid	[46]
H^+ / from 0 mV to +650 mV vs. Ag/AgCl, KCl (3 M)	Carbon fiber modified with rGO modified with syringaldazine	LR = 5.65–7.49 pH units; S = 60 mV pH $unit^{-1}$	(Human) HT-29 and HEK-293 cells	[47]
H_2O_2 / -200 mV vs. SCE	Glassy carbon modified with porous graphene modified with Pt nanoparticles	DL = 0.02 nM; LR1 = 0.06 nM – 0.855 μM; LR2 = 8.48 μM – 0.649 mM; S = 5980 nA μM^{-1} cm^{-2}	(Rat) PC12 / Adenosine 5′- diphosphate	[48]
·NO / +800 mV vs. Ag/AgCl	Screen printed carbon modified with N-doped graphene sheets, DNA, Au nanoparticles and laminin	DL = 0.8 nM; LR = 2–500 nM; S = 860.9 μA μM^{-1} cm^{-2}	(Human) MCF-7 / L-Arginine	[49]
H_2O_2 / 0 mV vs. SCE	Glassy carbon modified with GO modified with Co-doped PdCu nanoparticles	DL = 1.2 nM; LR = 5 nM – 5.774 mM; S = 3.85 μA mM^{-1}	(Rat) PC12 / Ascorbic acid	[50]
H_2O_2 / +100 mV vs. Ag/AgCl, KCl (sat)	Glassy carbon modified with rGO modified with Au – Pd nanocubes	DL = 4 nM; LR = 5 nM – 1 mM; S = 259.6 mA M^{-1} cm^{-2}; RT = 4 s	(Human) MCF-7, MDA-MB-231 and T47D / Ascorbic acid	[51]
H_2O_2 / -300 mV vs. SCE	Glassy carbon modified with chitosan and rGO modified with hemin-capped biomineralized gold nanoparticles	DL = 9.3 nM; LR1 = 50 nM – 1 μM; LR2 = 1 μM – 1 mM; S1 = 0.49 μA μM^{-1}; S2 = 0.03 μA μM^{-1}; RT = 50 s	(Human) HeLa / Ascorbic acid	[52]
Glutamate / +10 mV (drain – source) and + 100 mV (gate – source)	Field effect transistor with metabotropic glutamate receptor- modified rGO as gate	DL = 1 fM; LR = 1 fM – 100 pM	(Rat) primary hippocampus neurons	[53]
H_2O_2 / -200 mV vs. Ag/AgCl, KCl (sat)	Carbon fiber modified with rGO modified with Pt-Pd nanoparticles	DL = 0.3 μM; LR = 1–35 μM; S = 0.98 nA μM^{-1}	(Mouse) RAW 264.7 / Lipopolysaccharide	[54]

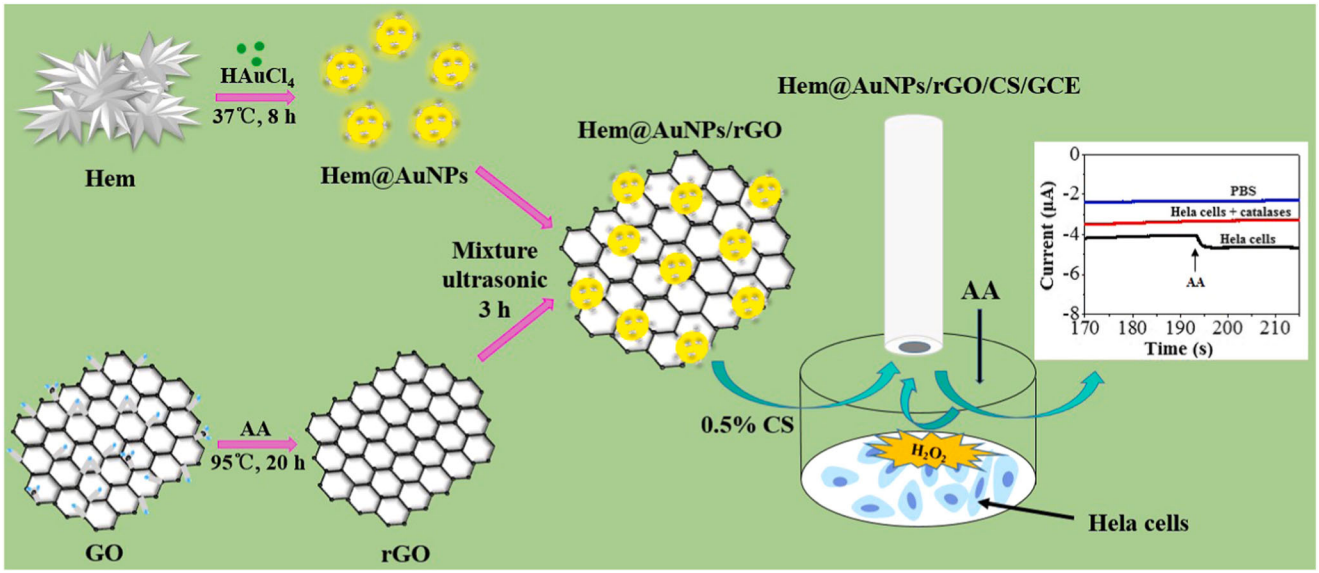

Fig. 1 Electrochemical sensor based on rGO for the detection of H_2O_2 in the extracellular space of HeLa cancer cells; Important to note, rGO (obtained by the chemical reduction of GO) was decorated with Au nanoparticles carrying hemin (Hem@AuNPs) and mixed with chitosan (CS) before being deposited onto a glassy carbon electrode (GCE). The resulting electrochemical sensor (Hem@AuNPs/rGO/CS/GCE) was used to measure H_2O_2 released by HeLa cancer cells following their stimulation with ascorbic acid (AA). Reprinted from Wang W, Tang H, Wu Y, Zhang Y, Li Z. Highly electrocatalytic biosensor based on Hemin@AuNPs/reduced graphene oxide/chitosan nanohybrids for non-enzymatic ultrasensitive detection of hydrogen peroxide in living cells. Biosens Bioelectron. 2019;132:217–223, with permission from Elsevier

As already mentioned, GBMs are most often combined with other electrocatalysts when building electrochemical sensors for living cells. About half of the reviewed sensors combine GBMs with noble metals. This is not a surprise considering the excellent electrocatalytic properties of these metals. While most sensors were built using one single noble metal, there are also sensors which were built using two (e.g. Pd and Pt [43]) or even three noble metals (e.g. Au, Pt, and Pd [46]). Several approaches were used to obtain the graphene – noble metal nanocomposites. Electrochemical deposition of the noble metal nanoparticles (e.g. Pt nanoparticles [20, 28, 29, 32, 33] or Au nanoparticles [30–32]) onto graphene-modified electrodes is one of them. Solution phase synthesis [25, 43] and metal sputtering [27] were also used to obtain the graphene – noble metal nanocomposites. Few oxides (e.g. CeO_2 [23] and Fe_3O_4 [21, 42]), Fe-containing macrocycles (e.g. Fe(III) meso-tetra (4-carboxyphenyl) porphyrin [26], and Fe(II) phthalocyanine [45]), and biomacromolecules (e.g. HRP [31] and metabotropic glutamate receptor [53]) were also used in combination with GBMs to build electrochemical sensors for investigating living cells. Doping is another way to improve the electrocatalytic properties of graphene [64]. Therefore, graphene doped with P [38] or co-doped with N and B [14] or N and S [13] was also explored to build electrochemical sensors. These devices are remarkable because of their relative simplicity as compared to sensors made with additional electrocatalysts.

Analysis of column 3 of Table 1 reveals that electrochemical sensors made with GBMs are characterized by a wide range of analytical performances even when made for the detection of the same analyte. One important question is whether these analytical performances are good enough or not. Unfortunately, there is no consensus regarding the physiological concentration of H_2O_2 and ·NO, the two analytes most often detected. A recent review puts the physiological extracellular H_2O_2 concentration range in between 100 nM and 1 μM and the supraphysiological extracellular H_2O_2 concentration above 10 μM [65]. Judged based on their lower detection limit, the vast majority of the H_2O_2 sensors presented in Table 1 are suitable for investigating these physiological H_2O_2 concentrations, while two sensors are suitable to observe supraphysiological H_2O_2 concentrations only. Analysis of several independent lines of evidence suggested the physiological ·NO concentration range to be 100 pM (or below) up to 5 nM [66]. This physiological ·NO concentration range can be measured with only half of the ·NO sensors listed in Table 1. The smallest detection limit for the detection of H_2O_2 and ·NO was 20 pM [48] and 55 pM [26], respectively. Furthermore, the sensors are very often characterized by extended linear ranges (e.g. 3–4 orders of magnitude). These ranges facilitate the exploitation of the sensors to advantageously observe both physiological and non-physiological analyte concentrations. Moreover, they also open the way for other applications, such as the detection of H_2O_2 in environmental samples (in which higher H_2O_2 concentrations have to be expected). The practical use of a couple of sensors is a little bit complicated by signals which show two linear ranges. The response time of the sensors is most often in the seconds

range. This response time allows using the sensors for monitoring the dynamics of the analyte release by the cells (while most other analytical methods are too slow to do the same). The relative standard deviation characterizing the sensors made with GBMs was in between 1.7% [38] and 8.2% [21] indicating good reproducibility of the sensor fabrication procedures. Unfortunately, it is not yet clear if these sensors can be reproducibly fabricated also in different laboratories, using materials from different sources. Most of the sensors retained at least 90% of their initial analytical signal after being stored (in various conditions) for time periods ranging from 7 days to 90 days. Only few sensors [20, 29, 33, 34, 36, 46, 48] were reported to retain less than 90% (72–87%) of their initial analytical signal after being stored for time periods ranging from 7 days to 30 days.

Concerning the used cellular models, about 25 models were studied using graphene-based electrochemical sensors. The cells originate from both humans and animals. Most of the investigated human cell lines are derived from different cancers: cervical (HeLa), liver (HepG2, SMMC-7721, or Hep3B), colon (HT-29), breast (HBL-100, MDA-MB-231, MCF-7, T47D, or MD-435), brain (U87), blood (CCRF-CEM, HL-60, or K562) or lung (A549). The preference of the authors for cancer cells reflects the common and standard procedure for in vitro cell biology investigations based on the reliable growth and easy-to-handle protocols of tumor-derived cell lines [67, 68]. Furthermore, cancer is among the leading causes of death worldwide [69] and, in comparison to normal cells, cancer cells are characterized by an increased H_2O_2 production rate [70]. Next to these models, immortalized endothelial (HUVEC), epithelial (HBL-100), kidney (HEK293), and liver cells (LO2) were also investigated, as well as primary neutrophils. The investigated animal-derived cell lines were less numerous, clearly indicating a preference for cellular models which are relevant for human pathologies. The animal cells explored were skin cells (JB6-C30), cardiac cells (H9C2), macrophages (RAW 264.7), primary neurons (from rat hippocampus), and cancer cells (PC12 or B16-F10).

Figure 2 shows typical results obtained at cellular level with an electrochemical ·NO sensor built using graphene. A glassy carbon electrode, modified with 3D reduced graphene hydrogel and Au nanoparticles, was used to detect the ·NO released by normal mouse skin cells (JB6-C30) and mouse melanoma cells (B16-F10) following stimulation with acetylcholine (that activates nitric oxide synthase) [24]. The observed current signals indicate that: *i.)* detectable ·NO release occurs 20 s after stimulation of the cells with acetylcholine (and after a current spike not related to ·NO release) and lasts roughly 1 min (see Fig. 2b), *ii.)* the magnitude of the ·NO release is dependent on the concentration of acetylcholine used to stimulate the cells (see Fig. 2c and f), and *iii.)* melanoma cells release more ·NO than normal skin cells in the same experimental conditions (see Fig. 2c vs. Figure 2f).

There are also some limitations which are difficult to deduce from Table 1 but worth mentioning in order to present a correct picture of the electrochemical sensors made with GBMs and used to investigate cells:

i Although the distance in between the cells and the electrochemical sensor is very important (because compounds are secreted locally in moderate concentrations but are quickly diluted after release), this distance was not controlled in a precise manner in many of the works mentioned in Table 1. Two very different approaches were used in the few studies in which this distance was controlled. The first approach consists of growing the cells directly on the surface of the sensor, thus reducing the distance in between cells and sensor to a well-controlled minimum [26, 49, 53]. The second approach consists of using Scanning Electrochemical Microscopy (SECM) to control the distance between cells and sensor [47]. The first approach requires no additional equipment and, thus, has the advantage of simplicity. However, cells are usually kept in contact with the sensor surface only for a very short period of time before the actual experiments. These short periods of time are not enough for the cells to properly adhere to the surface and to build intercellular structures (such as tight junctions). In other words, the first approach tends to use cells in a state that is not really physiological. SECM allows the reproducible positioning of microelectrodes to known distances from the investigated sample (e.g. cell-covered culture ware). It also allows moving / scanning the microelectrode to investigate several points of interests (e.g. several individual cells, or groups of cells, depending on the size of the microelectrode). However, it requires a relatively bulky micropositioning system which adds to the complexity and price of the experimental setup.

j The electrochemical sensors which detect H_2O_2 by electroreduction of H_2O_2 (i.e. the majority of the sensors detailed in Table 1) perform well only in the absence of O_2 (because the electroreduction of O_2 can interfere with the electroreduction of H_2O_2). In the same time, living cells perform in a normal manner only in normoxic conditions. Hypoxic conditions have an important impact on both cancer cells and normal cells. Therefore, working in hypoxic conditions in order to preserve the selectivity of the electrochemical sensor for the detection of H_2O_2 is clearly not the best option. These facts are neglected in several studies listed in Table 1 (and also in Table 2, see below).

k The exact impact of the GBM integrated into the electrochemical sensor on the analytical performances of the sensor is not always clear (because measurements carried out with sensors made without the GBM are sometimes missing). When this impact was evaluated, it was found that

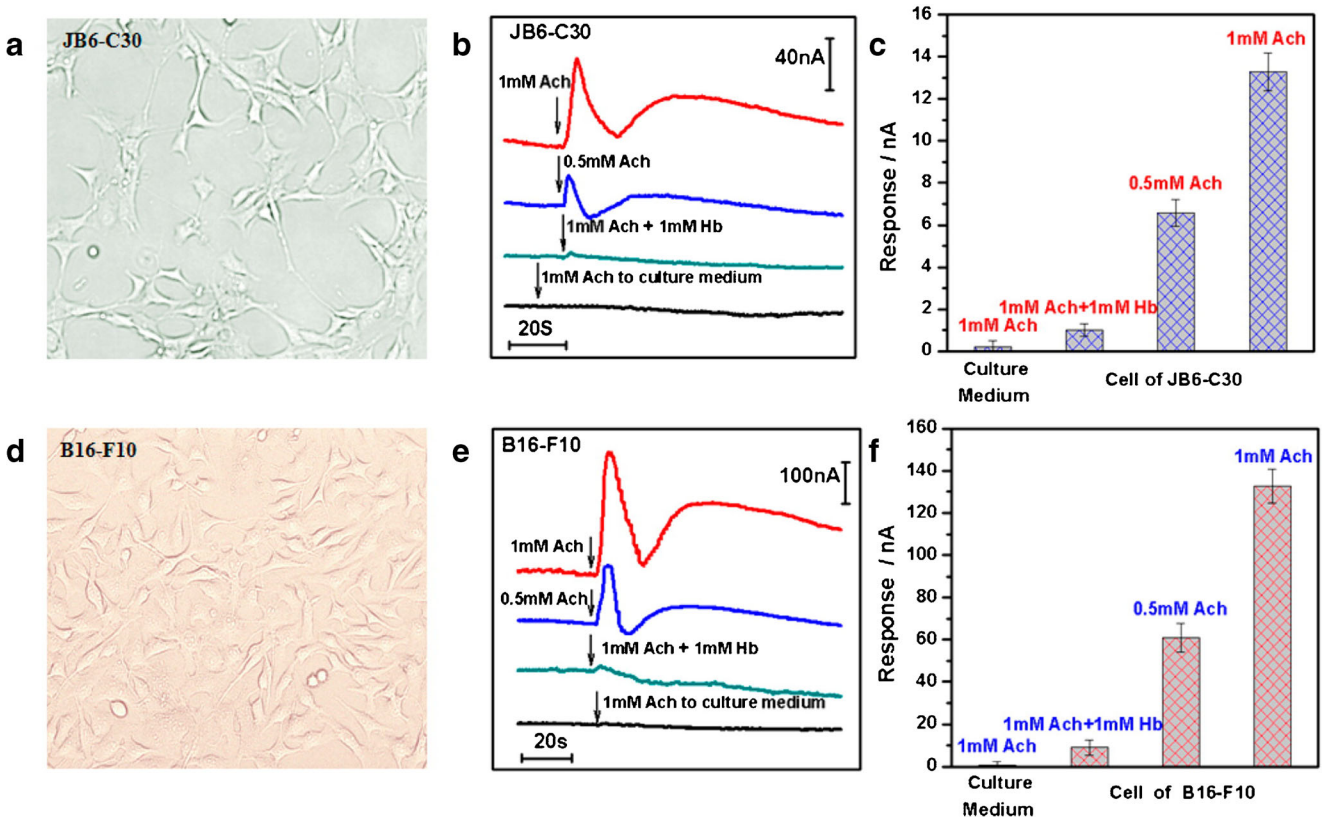

Fig. 2 Typical results obtained while investigating living cells with an electrochemical sensor built using a 3D reduced graphene hydrogel; The figure shows pictures of JB6-C30 normal skin cells (**a**) and B16-F10 melanoma cells (**d**), the time evolution of the ·NO concentration-proportional current signal before and after stimulation of the cells with acetylcholine (Ach) or acetylcholine and hemoglobin mixtures (Ach + Hb) (**b** and **e**), and a comparison of the ·NO concentration-proportional current signal observed in different experimental conditions (**c** and **f**). Reprinted with permission from Li J, Xie J, Gao L, Li CM. Au nanoparticles–3D graphene hydrogel nanocomposite to boost synergistically in situ detection sensitivity toward cell-released nitric oxide. ACS Appl Mater Interfaces. 2015;7:2726–2734. Copyright (2015) American Chemical Society

using GBMs can lead to an increase from 20% (when deposited as a 2D layers) [20] to 600% (when deposited as a 3D layer) [24] of the electrochemically active surface area. However, there are several other materials than graphene which can be used to increase the area of the electrochemically active surface (e.g. carbon nanotubes, conducting polymers, porous metal layers, etc.).

l The selectivity of the developed electrochemical sensors was often rather superficially investigated. For example, current signals generated by 0.1 mM H_2O_2 were compared to those generated by 1.0 mM uric acid, 0.5 mM ascorbic acid and 1.0 mM glucose. Since currents generated by 0.1 mM H_2O_2 were much higher than those generated by the tested concentrations of possibly interfering compounds, the developed sensor was declared selective enough [13, 20]. However, cells usually produce H_2O_2 concentrations much smaller than 0.1 mM in their extracellular space. The selectivity of many ·NO sensors was also rather superficially investigated. For example, current signals generated by 1–2 μM ·NO were compared to those generated by 1–2 μM of uric acid, ascorbic acid, dopamine, H_2O_2 or L-Arginine [24, 26] while some of these compounds can be present in the extracellular space in much higher concentrations. A rigorous test of selectivity must compare current signals given by relevant concentrations of the targeted analyte and relevant concentrations of the possibly interfering compounds.

m The results obtained using the graphene-based electrochemical sensors were seldom confirmed with additional analytical methods. While some of the data (such as those obtained from individual or a low number of cells) might be difficult to confirm with other analytical methods, many results (such as those obtained from millions of cells) can be confirmed with classic analytical methods (such as spectrophotometry). In order to see electrochemical sensors more widely accepted in cell biology laboratories, it is important to show that these tools can at least deliver the same information as more traditional analytical tools while being better in some aspects (e.g. sensitivity, response time, etc.)

n The number of experiments in which electrochemical sensors made with GBMs are used to investigate living cells is

usually very low. Several studies present 1–2 signals recorded at cellular level. Considering that such sensors (although not necessarily made with GBMs) have been around for a while, their utility in the investigation of biological questions must be more convincingly proved in order for this field to progress.

Electrochemical sensors built with non-graphene 2D materials

GBMs are not the only 2D materials used to develop electrochemical sensors for investigating living cells. Figure 3 shows a scheme with the main steps of making an electrochemical sensor that is based on MoS_2 and trimetallic (Au-Pd-Pt) nanoflowers, and that was used for the detection of H_2O_2 released from MCF-7 breast cancer cells [77]. The analytical performances of the sensor are listed in Table 2 together with details about other electrochemical sensors made with non-graphene 2D materials.

As one can observe by comparing Tables 1 and 2, the electrochemical sensors made with non-graphene 2D materials share many similarities with the electrochemical sensors made with GBMs. For example, both sensor types were most often built on glassy carbon electrodes and target H_2O_2 that is detected by making use of constant potential amperometry and about the same, rather negative, potentials. Moreover, just as the electrochemical sensors built with GBMs, sensors built with non-graphene 2D materials commonly rely on additional electrocatalysts (e.g. noble metal nanorods and nanoflowers). Obviously, there are also differences between the two sensor types. For instance, there is no sensor made with non-graphene 2D material for the detection of ·NO in the extracellular space, while ·NO is quite often targeted by the sensors made with GBMs (see Table 1). Thus, it is not yet clear whether non-graphene 2D materials are suitable for building electrochemical ·NO sensors or not.

MoS_2, a transition metal dichalcogenide (TMD), is the non-graphene 2D material most frequently used to build electrochemical sensors for the investigation of living cells. Electrochemical sensors made with this material but not necessarily used to investigate living cells were reviewed elsewhere [85]. Three other TMDs (WS_2 [72], CoS_2 [80] and $Mo_{0.75}W_{0.25}S_2$ [83]) and an MXene (Ti_3C_2 [81]) were also used to make electrochemical sensors to investigate living cells. It is difficult to say if one of these novel 2D materials is better for building electrochemical sensors than the other because the number of electrochemical sensors made with them is still too small and the devices are built in very different manners (e.g. they are mixed with different electrocatalysts).

Electrochemical sensors made with non-graphene 2D materials have, in generally, analytical performances (i.e. limit of detection and linear range) which make them suitable for monitoring both physiological and supraphysiological concentrations of H_2O_2 in the extracellular space of living cells. The smallest detection limit reported for a H_2O_2 sensor made with a non-graphene 2D material was 0.3 nM [77]. This value is an order of magnitude larger than the smallest detection limit reported for H_2O_2 sensors made with GBMs (20 pM [48]). However, sensors were not made in similar ways in order to allow a meaningful direct comparison of their analytical performances. The relative standard deviation characterizing the sensors made with non-graphene 2D materials was in between 3.4% [75] and 8.6% [78]. This reproducibility is quite similar to that of the sensors made with GBMs (see Section 2). Most of the sensors made with non-graphene 2D materials retained at least 90% of their initial analytical signal after being stored (in different conditions) for time periods ranging from 7 days [82] to couple of weeks [74, 75, 78]. Only one sensor [76] was reported to retain less than 90% (85%) of its initial analytical signal after being stored for a time period of 30 days. Thus, sensors made with non-graphene 2D materials seem as stable as those made with GBMs.

Just as the electrochemical sensors made with GBMs, the electrochemical sensors made with TMDs and MXenes were used to investigate a variety of cellular models of both human and animal origin. Human cell lines were mainly derived from different cancers: breast (MCF-7 and MDA-MB-231), lung (A549), cervical (HeLa), or liver (HepG2). The animal cell lines tested were instead macrophages (RAW 264.7), fibroblasts (NIH-3 T3), cardiomyocytes (H9C2), mammary carcinoma cells (4 T1), or myeloma cells (SP2/0).

Figure 4 shows typical results obtained at cellular level with an electrochemical H_2O_2 sensor built using MoS_2. A glassy carbon electrode was modified first with a mixture of MoS_2 nanosheets and Fe_3O_4 nanoparticles coated with ZIF-8 metal organic framework nanoparticles and then with Au nanoflowers in order to obtain the H_2O_2 sensor [82]. Before using this H_2O_2 sensor at cellular level, fluorescence microscopy and dihydroethidium (a probe sensitive to reactive oxygen species) were used to demonstrate that the selected cells (H9C2 rat cardiomyocytes) produce H_2O_2 following stimulation with ascorbic acid (see Fig. 4a and b). Subsequently, the electrochemical H_2O_2 sensor was used to detect the H_2O_2 released by the cells following stimulation with ascorbic acid (see Fig. 4c). The results, obtained with fluorescence microscopy and electrochemistry, indicate that: *i.)* ascorbic acid induces the production of reactive oxygen species (such as H_2O_2 and $O_2^{\cdot-}$) in the intracellular space of the selected cells (see Fig. 4a and b), *ii.)* the H_2O_2 produced in the intracellular space shows up very fast also in the extracellular space of the cells (see Fig. 4c), and *iii.)* judged on their morphology (see Fig. 4d), the cells do not suffer during the electrochemical experiment (which is not very surprising taking into account the short duration of the electrochemical experiment, only about 200 s).

Table 2 Electrochemical sensors made with non-graphene 2D materials and used to investigate living cells (Observations: Sensors are listed in chronological order. DL, LR, S, and RT stay for detection limit, linear range, sensitivity, and response time, respectively)

Analyte / Applied potential	Sensor structure	Analytical performances	Investigated cells / Stimulus	Ref.
H_2O_2 / -250 mV vs. SCE	Glassy carbon modified with MoS_2 particles	DL = 2.5 nM; LR1 = 5.0–100 nM; S1 = 2.58×10^3 mA cm^{-2} M^{-1}; LR2 = 100 nM - 100 μM; S2 = 160 mA cm^{-2} M^{-1}; RT = 5 s	(Mouse) RAW 264.7 / fMLP	[71]
H_2O_2 / -250 mV vs. Ag/AgCl	Carbon fibers modified with 3D networks of WS_2 nanosheets	DL = 2 nM; LR = up to ~150 μM	(Mouse) RAW 264.7 cells; (rat) primary hippocampal neurons / fMLP; epidermal growth factor (EGF)	[72]
H_2O_2 / -250 mV vs. SCE	Glassy carbon modified with MoS_2 nanosheets carrying PtW nanocrystals	DL = 5 nM; LR = 1 μM – 0.2 mM; S = 1.71 μA $μM^{-1}$ cm^{-2}; RT = 5 s	(Mouse) 4 T1 / fMLP	[73]
H_2O_2 / -550 mV vs. SCE	Glassy carbon modified with MoS_2, Au nanorods, and catalase	DL = 0.1 μM; LR = 0.5 μM – 0.2 mM; S = 187 mA M^{-1} cm^{-2}; RT = 2.5 s	(Mouse) SP2/0 / fMLP	[74]
H_2O_2 / -600 mV vs. SCE	Glassy carbon modified with ultrathin MnO_2 nanosheets	DL = 5 nM; LR = 25 nM – 2 μM; S = 3261 mA M^{-1} cm^{-2}; RT = 3 s	(Mouse) SP2/0 / Ascorbic acid	[75]
H_2O_2 / -150 mV vs. Ag/AgCl	Stainless steel coated with Au and then modified with MoS_2 nanosheets and Pt nanoparticles	DL = 0.69 μM; LR = 1–100 μM; S = 0.004 μA $μM^{-1}$; RT = 2 s	(Human) HeLa / PMA	[76]
H_2O_2 / 0 mV vs. Ag/AgCl	Screen printed carbon modified with MoS_2 nanosheets carrying trimetallic nanoflowers	DL = 0.3 nM; LR = 1–100 nM; S = 0.059 μA nM^{-1}; RT = 2.5 s	(Human) MCF-7 / PMA	[77]
H_2O_2 / -100 mV vs. SCE	Glassy carbon modified with N-doped carbon nanowires carrying MoS_2 nanosheets	DL = 0.73 μM; LR = 2–500 μM; RT = 15 s	(Human) A549 / fMLP	[78]
H_2O_2 / -500 mV vs. SCE	Carbon cloth modified with MoS_2 nanosheets	DL = 1 μM; LR1 = 5–235 μM; LR2 = 435 μM – 3 mM; S1 = 5.3 mA mM^{-1} cm^{-2}; S2 = 3.6 mA mM^{-1} cm^{-2}; RT = 3 s	(Human) A549 / PMA	[79]
H_2O_2 / -620 mV vs. Ag/AgCl, KCl (sat)	Carbon cloth modified first with CoS_2 nanosheets and then with $NiCo_2S_4$	DL = 2 nM; LR = 13 nM – 2.1 mM; S = 1.49 μA $μM^{-1}$ cm^{-2}; RT = 4 s	(Murine) RAW 264.7 / Lipopolysacharide	[80]
$O_2^{\cdot-}$ / +750 mV vs. Ag/AgCl, KCl (3 M)	Glassy carbon modified with Ti_3C_2 (MXene) nanosheets carrying $Mn_3(PO4)_2$ nanoparticles	DL = 0.5 nM; LR = 2.5 nM – 14 μM; S = 7.86 mA mM^{-1} cm^{-2}; RT = 20 s	(Human) HepG2 / Zymosan	[81]
H_2O_2 / -550 mV vs. Ag/AgCl, KCl (sat)	Glassy carbon modified first with a mixture of MoS_2 nanosheets and Fe_3O_4 nanoparticles coated with ZIF-8 metal organic framework nanoparticles and then with Au nanoflowers	DL = 0.9 μM; LR1 = 5 μM – 15 mM; LR2 = 15–120 mM; S1 = 0.0171 μA $μM^{-1}$; S2 = 0.00417 μA $μM^{-1}$	(Rat) H9C2 / Ascorbic acid	[82]
H_2O_2 / -600 mV vs. Ag/AgCl, KCl (3 M)	Glassy carbon modified with $Mo_{0.75}W_{0.25}S_2$ nanoflowers	DL = 0.3 μM; LR = 0.4 μM – 10 mM; S = 1290 μA mM^{-1} cm^{-2}; RT = 3 s	(Human) MDA-MB-231; MCF-7; and HeLa; (murine) NIH-3 T3 / PMA	[83]
H_2O_2 / -300 mV vs. Ag/AgCl	Glassy carbon modified with MoS_2 nanosheets grown onto Mo_2C nanorods	DL = 0.2 μM; LR = 0.2 μM – 6.6 mM; S = 1080 μA mM^{-1} cm^{-2}	(Human) MDA-MB-231 and red blood cells / PMA	[84]

Most limitations mentioned in relation to graphene-based electrochemical sensors are also valid for the electrochemical sensors in which graphene was replaced with other 2D materials. The distance in between the investigated cells and the

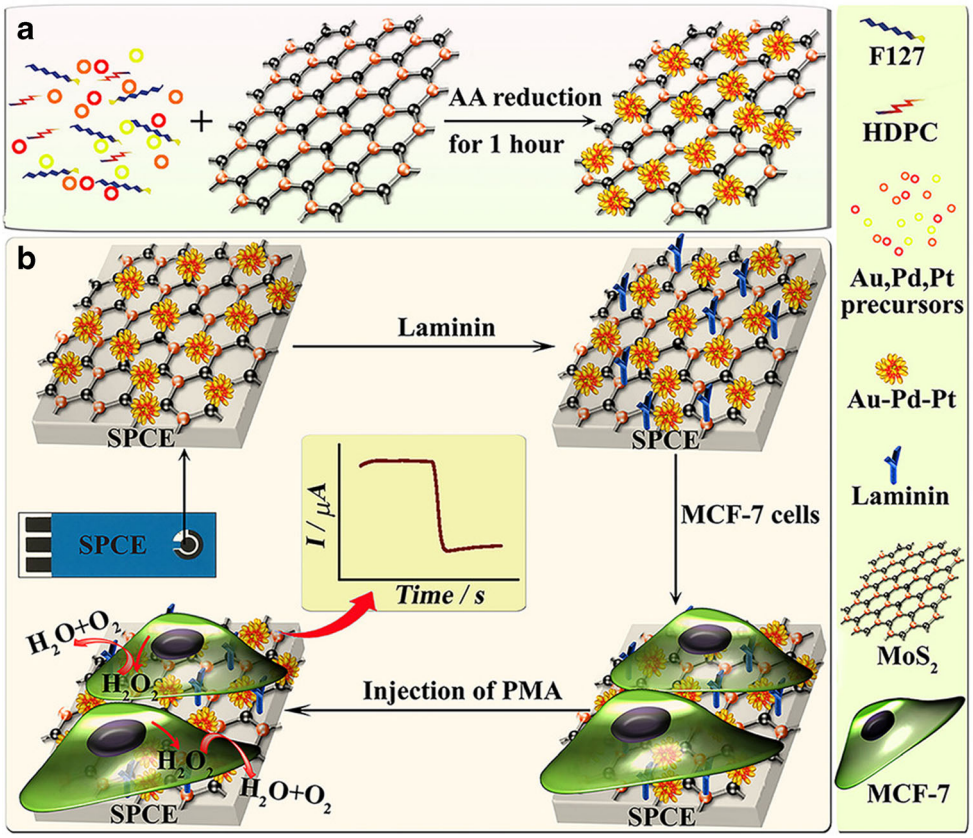

Fig. 3 Electrochemical sensor based on MoS_2 for the detection of H_2O_2 in the extracellular space of living cells; Important to note, the MoS_2 nanosheets were decorated with Au-Pd-Pt nanoflowers before being deposited onto the screen printed carbon electrode (see panel **a**) and the investigated cells (MCF-7) were grown directly onto the surface of the sensor before being stimulated to generate H_2O_2 by using PMA (see panel **b**). Reprinted with permission from Dou B, Yang J, Yuan R, Xiang Y. Trimetallic hybrid nanoflower-decorated MoS_2 nanosheet sensor for direct in situ monitoring of H_2O_2 secreted from live cancer cells. Anal Chem. 2018;90:5945–5950. Copyright (2018) American Chemical Society

sensor was very seldom controlled. Cells were often investigated in suspension without regard if this was their physiological state or not. In the best-case scenario, cells were grown directly onto the sensor surface (e.g., in refs. [72, 77]), thus, reducing the distance in between cells and sensor to minimum. H_2O_2, the analyte most often targeted, was still detected through its electrochemical reduction at potentials were the reduction of O_2 also occurs (e.g., −620 mV). Some of the sensors were made using complex mixtures of several nanomaterials but the exact role of each nanomaterial was not always investigated. Therefore, one is left with the impression that not all nanomaterials adopted to fabricate the device are really needed in the structure of the sensors. Some of the electrochemical signals recorded in the presence of the targeted analyte are confusing. For example, although $O_2^{\cdot -}$ is known to rapidly disproportionate into H_2O_2 and O_2, the current response of some amperometric $O_2^{\cdot -}$ sensors did not show signs of this process during calibration [81]. Results obtained with the electrochemical sensors made with non-graphene 2D materials were seldom compared with results obtained with widely accepted analytical methods. However, in the very few studies which contain such a comparison (e.g. in [82]), a good match of the results was observed. Finally, the number of experiments involving living cells is most often low. However, there are few studies which take into work both cancer cells and normal cells in order to show that the electrochemical sensors made with 2D materials are able to reveal differences in between these two cell types.

Electrochemical sensors based on 2D materials which are wearable or suitable for in vivo use

Results obtained using cell cultures are very valuable as they provide important information on the mechanism of action of a drug candidate, novel material or environmental pollutant. However, these in vitro results must be confirmed using more complex biological systems (e.g. 3D organoids, tissue slices, etc.) and ultimately in vivo experiments. Therefore, it is important to evaluate the extent to which electrochemical sensors made with 2D materials are suitable to investigate also biological systems which are more complex than cell cultures. We carried out this evaluation in two steps which are presented in this and the next section of the review. First, we searched and analyzed the literature on electrochemical sensors which were already used on the surface of different body parts (i.e. as wearable sensor) or in vivo (i.e. as implanted sensor). Second, we searched and analyzed the relatively vast literature on the biocompatibility of the 2D materials most often used to build electrochemical sensors (e.g. graphene, MoS_2, etc.). The most important findings related to the biocompatibility of the 2D

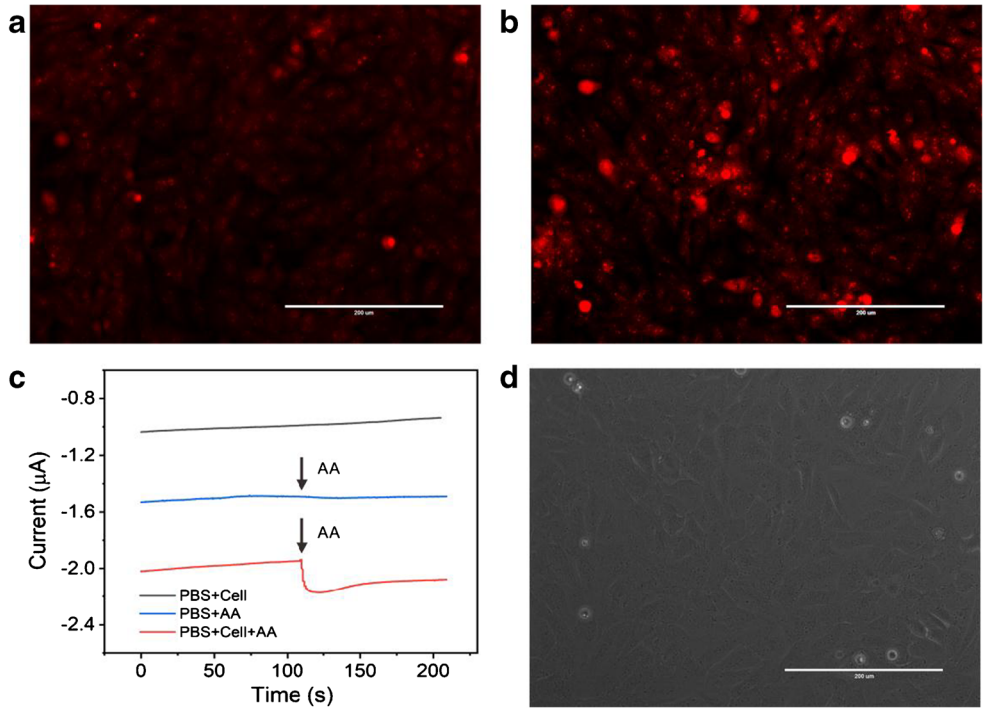

Fig. 4 Typical results obtained while investigating living cells with an electrochemical sensor built using MoS_2; The figure shows pictures of H9C2 rat cardiomyocytes loaded with dihydroethidium before (**a**) and after (**b**) stimulation with ascorbic acid, the time evolution of the H_2O_2 concentration-proportional current signal before and after stimulation of the cells with ascorbic acid (**c**), and H9C2 rat cardiomyocytes after the experiment involving the electrochemical H_2O_2 sensor (**d**). Reprinted from Lu J, Hu Y, Wang P, Liu P, Chen Z, Sun D. Electrochemical biosensor based on gold nanoflowers-encapsulated magnetic metal-organic framework nanozymes for drug evaluation with in-situ monitoring of H_2O_2 released from H9C2 cardiac cells. Sens Actuators B Chem. 2020;311:127909, with permission from Elsevier

materials are detailed in the next section. Thus, this and the next section together give us a peek into the future of electrochemical sensors made with 2D materials and used to investigate biological systems.

2D materials combine good electrical conductivity with flexibility and mechanical robustness, properties which make such materials especially suitable for developing electrochemical sensors to be worn in intimate contact with the rugged surfaces of different body parts. Table 3 lists details about the electrochemical sensors made with 2D materials which were already tested as wearable sensor.

Relatively few wearable electrochemical sensors have been made using 2D materials up to now. Interestingly, while the sensors listed in Tables 1 and 2 (i.e. the sensors used at cellular level) target mainly H_2O_2 and ·NO, the wearable electrochemical sensors made with 2D materials target glucose first of all. Monitoring blood glucose concentration is a very important part of managing *diabetes mellitus* (as discussed, for example, in [95]). In other words, wearable electrochemical sensors tend to target molecules important for disease management rather than molecules important for understanding disease mechanism.

As one can observe in the second column of Table 3, GBMs are the 2D materials used to make wearable electrochemical sensors. The role of GBMs in these sensors is very variable. While in some wearable sensors they get a major role [86, 87] in other wearable sensors they have only a minor role [89, 90]. Just as in the sensors for investigating living cells (Tables 1 and 2), GBMs are most often combined with nanomaterials made of noble metals in wearable sensors as well, and, as a novelty compared to the previously presented sensors, with an oxidase that converts glucose and O_2 to gluconolactone and H_2O_2 (i.e. GOx).

The analytical performances of wearable electrochemical sensors made with 2D materials are usually not very thoroughly described. Papers published about such sensors focus on the selection of the appropriate materials for building the sensor, the method to interface it with the body, and the method to collect the body fluid to be analyzed rather than the analytical performances of the sensor itself. However, the performances of the wearable electrochemical sensors seem fit for purpose (as authors aimed for proof-of-principle studies only). The glucose sensors integrated into contact lenses were proved to be stable for 24 h [88] or 48 h [91] while those integrated into patches to be worn on the skin were proved to retain at least 85% (typically more than 90%) of their initial signal for time periods ranging from 6 days to 10 days [87, 89, 92, 94].

The 2D material-based wearable electrochemical sensors developed so far were made to work either on the skin (e.g. of the forearm) or placed on the eyeball, while one single sensor has been placed onto tooth enamel [86]. Therefore, they report on the concentration of the analyte of interest in sweat, tears, interstitial fluid, or saliva.

An important problem that must be solved with all wearable electrochemical sensors is applying potentials to and reading signals from the sensor in a convenient (i.e. portable) way. So far, two approaches were used to solve this problem. The simplest approach was to rely on miniaturized potentiostats which, although wired to the sensor, do not impede the users in carrying out their normal duties [87, 89, 94]. The more advanced approach was to wirelessly power the sensor (through an antenna and inductive coupling) and wirelessly read sensor signals as a resonance frequency shift or change in the luminous intensity of a LED integrated in parallel with the sensor [86, 88, 91].

Wearable electrochemical sensors rely very much on the relatively simple chemical composition of sweat, tears, interstitial fluid, or saliva. For example, these body fluids are not containing large concentrations of proteins. The situation is completely different in case of the electrochemical sensors to be used in vivo. Such sensors must not only "survive" implantation into tissue but must also perform well in an environment of great chemical complexity. Moreover, they must also cause minimal tissue damage and must be accepted by the immune system of the host. It is still very difficult to build such electrochemical sensors. This explains why Table 4 lists details about only a handful of electrochemical sensors made with 2D materials which were already used in vivo.

While electrochemical sensors used at cellular level most often target the detection of H_2O_2 (see Table 1), and wearable electrochemical sensors most often target the detection of glucose (see Table 2), electrochemical sensors made with 2D materials and used in vivo bring into the picture the detection of dopamine. Dopamine is a biogenic amine neurotransmitter of which concentration in the central nervous system is controlled by specialized (i.e. dopaminergic) neurons. Altered levels of dopamine in brain are associated with several human neurological disorders, e.g. Parkinson's disease [101].

Electrochemical sensors made with 2D materials and used in vivo were most often built using carbon fiber microelectrodes characterized by small lateral dimension (e.g. 7 μm) in order to not cause significant tissue damage and substantial immune response when the sensors are implanted. GBMs were the 2D materials most often used to build such sensors. Important to mention, the in vivo electrochemical determination of dopamine with carbon fiber microelectrodes is around already for decades (see, for example, in [102]). While 2D materials do not facilitate the detection of new analytes they do increase the sensitivity of the carbon fiber microelectrode to the previously detected analytes.

Murine brain is the organ most often investigated using electrochemical sensors made with 2D materials. Unfortunately, it is not uncommon that a rather superficial study on the selectivity of the sensor is followed by recording only few signals with the sensor implanted in the brain. In depth in vivo investigations with the newly developed sensors are most often missing.

Studies carried out up to now with wearable or in vivo sensors made with 2D materials are short term, proof of principle studies. As such, many of these studies [86, 88, 90, 91, 94, 96, 98–100] disregard sensor performance degradation due to biofouling (i.e. due to the accumulation of proteins, cells and other biological materials onto the surface of the sensor). Other studies rely on classic solutions (e.g. on Nafion outer layers [87, 89, 92, 97]) to protect the sensing layer (e.g. during implantation) and to minimize problems related to biofouling. For converting its electrochemical signal into an analyte concentration, the wearable or in vivo sensor is usually calibrated in vitro, just before being placed onto or into the body (e.g. by using artificial sweat or artificial tear samples with known analyte concentrations [87, 91, 92]). Obviously, this procedure works well only if the sensor is characterized by good stability in the conditions of use. In order to obtain biologically relevant analyte concentrations (e.g. in order to obtain the blood glucose concentration from the glucose concentration measured in sweat), such pre-calibration experiments are completed with analyte concentration measurements made with standard methods (e.g. with blood glucose measurements made with commercial glucose meters) [87, 89, 94]. However, once the correlation in between the analyte concentration in blood and the analyte concentration in the alternative sample (e.g. sweat, tear, saliva, etc.) is firmly established, using the standard method in parallel with the pre-calibrated sensor is not needed anymore. Standard methods to measure the concentration of the analyte of interest (e.g. the already mentioned commercial glucose meters) can also be used to carry out the one-point calibration of in vivo sensors [97]. This method still uses data (e.g. sensor sensitivity) from in vitro pre-calibration experiments.

Will we witness the integration of a 2D material-based electrochemical sensor into a commercial wearable device anytime soon? Is it possible to use 2D material-based electrochemical sensors for in depth biological studies? In order to answer these questions, in the next section we shortly review studies on the biocompatibility of the most popular 2D materials used in the sensors mentioned in Tables 1, 2, 3, and 4.

Biocompatibility and biodegradation of 2D materials used to build electrochemical sensors

There are no 2D material-based electrochemical sensors on the market yet. This situation can in part be explained by the limited effort spent to investigate the biosafety and biocompatibility of 2D materials [103]. To accelerate the transition of 2D material-based devices (including electrochemical sensors) from laboratory prototypes to commercial products, it is of outmost importance to explore any potential unwanted effect triggered by any component of these devices. We also

Table 3 Electrochemical sensors made with 2D materials and used as wearable sensor (Observations: Sensors are listed in chronological order. DL, LR, S, and RT stay for detection limit, linear range, sensitivity, and response time, respectively)

Analyte / Applied potential	Sensor structure	Analytical performances	Body fluid / Body part	Ref.
H. pylori cells / alternative current was applied	Interdigitated gold electrodes carrying a graphene monolayer obtained by chemical vapor deposition (CVD) and modified with antimicrobial peptide	DL = 100 bacterial cells; LR = 100–10^6 cells; RT = 15 min	Saliva / Enamel of extracted tooth	[86]
Glucose / - 50 mV vs. Ag/AgCl	Hybrid material (consisting of graphene and Au nanoparticles on Au mesh) modified with Prussian Blue and glucose oxidase (GOx)	LR = 10 μM - 0.7 mM	Sweat / Skin on the inner forearm of healthy volunteers	[87]
Glucose / +100 mV (drain – source) and 0 mV (gate – source)	Field effect transistor with graphene gate that is modified with GOx	DL = 0.4 μM; LR = 1 μM – 10 mM	Tears / Eyeball of live rabbit	[88]
Glucose / -200 mV vs. Ag/AgCl	Porous Au modified first with Prussian Blue and then with graphene and GOx	LR = 10 μM - 1 mM	Sweat / Skin on the outer forearm of human subjects	[89]
Glucose / +400 mV vs. Ag/AgCl	Screen printed electrodes made with graphene ink and modified with Pt nanoparticles	LR = up to 0.75 mM; S = 23.58 μA mM^{-1} cm^{-2}	Interstitial fluid / Skin on the forearm of healthy human subjects	[90]
Glucose / 10 V_{rms}	Graphene modified with GOx and catalase	DL = 12.57 μM; LR = up to 1 mM; S = −22.72% mM^{-1}; RT = 1.3 s	Tears / Eyeball of live rabbit	[91]
Glucose / +350 mV vs. Ag/AgCl	Thin film Au electrode modified with rGO, Au-Pt alloy nanoparticles and GOx	DL = 5 μM; LR = up to 2.4 mM; S = 48 μA mM^{-1} cm^{-2}; RT = 20 s	Sweat / Skin on the inner wrist of human subjects	[92]
H_2O_2 / -700 mV vs. Ag/AgCl	Stainless steel microneedles modified with rGO and Pt nanoparticles	LR = up to 6 mM; S = 0.134 mA mM^{-1}	Interstitial fluid / Pig skin and living mice skin	[93]
Glucose / +200 mV vs. Ag/AgCl	rGO polyurethane composite fiber partially covered with Au nanowrinkles	DL = 500 nM; S = 140 μA mM^{-1} cm^{-2}	Sweat / Skin on the forehead of healthy human subjects	[94]

need to remember that 2D materials are relatively new candidates as biomaterials and the tissue/organ/body response upon their exposure is not yet fully understood or conclusive [103–106].

Studies on the biocompatibility of 2D materials have been carried out both in vitro and in vivo in the last decade, once the opportunity of using such materials for biomedical applications became clear [105, 107]. However, the determination of the common mechanisms of 2D material toxicity when in contact with biological systems is still a major challenge, as multiple parameters have to be considered leading to discrepancy in the present literature [103, 108]. Lateral dimensions, thickness, oxidation degree, surface chemistry (including surface functionalization), formulation and the biological system used to test the biocompatibility (cell lines differ one from another) will all contribute to the final output of the research [103, 109]. The consequence is that, although tempting, it is not correct to generalize on 2D materials biointeractions and biocompatibility.

It is worth to note also that electrochemical sensors are used to investigate biological systems for very different durations. Implantable sensors (Table 4) are inside the investigated tissue for days, wearable sensors (Table 3) are in contact with different body parts for hours, while sensors used to investigate cell cultures (Tables 1 and 2) are placed in the extracellular space for only couple of minutes (see Figs. 2b, e, and 4c). Biocompatibility studies, on the other hand, investigate in most cases biological effects occurring within hours and days. Therefore, in the way they are carried out today, these studies are highly and immediately important for implantable and wearable electrochemical sensors. They will gain importance also for sensors used to investigate cell cultures if the stability of such sensors will be improved and the sensors will be used to observe cell cultures for longer times.

One distinction that is necessary to make is between 2D-flakes (i.e. nanosheets in solutions) and 2D-films (i.e. surface-coatings, most often used in electrochemical sensors). In fact, the main safety concerns for GBMs come from their nanoforms, as nanosheet liquid suspensions or aerosols [104, 108, 110]. However, implanted devices containing 2D materials might release fragments into the body coming from degradation/delamination of the 2D-films. For these reasons, it is extremely important to carefully address the degradation of the composite materials/devices and the biodistribution of the fragments. If for graphene it is possible to find a wide and extensive literature about the biocompatibility of both flakes and 2D-films, for other recently introduced 2D-materials only few papers are addressing the issue [105]. In addition, 2D

Table 4 Electrochemical sensors made with 2D materials and used in vivo (Observations: Sensors are listed in chronological order. DL, LR, S, and RT stay for detection limit, linear range, sensitivity, and response time, respectively)

Analyte / Applied potential	Sensor structure	Analytical performances	Body part	Ref.
Dopamine / from −500 mV to +1 V vs. Ag/AgCl	Carbon fiber modified with poly(3,4-ethylene dioxythiophene) and GO	DL = 0.090 μM; LR = up to (at least) 10 μM; S = 43.12 nA μM^{-1}	Rat dorsal striatum	[96]
Glucose / -150 mV vs. Ag/AgCl	Printed Au modified with layers made of rGO, Pt and GOx	DL = 3.54 mg dL^{-1}; LR = up to 570 mg dL^{-1}; S = 0.354 nA mg^{-1} dL	Subcutaneous tissue on the posterior neck of rat	[97]
Dopamine / from −400 mV to +1 V vs. Ag/AgCl	Carbon fiber modified with a Cu_2S and rGO nanocomposite	DL = 24 nM; LR = 0.1–20 μM; S = 22.34 pA μM^{-1} μm^{-2}	Brain of *Drosophila melanogaster*	[98]
H^+ / open circuit potential vs. Ag/AgCl	Stainless steel modified first with MoS_2 nanosheets and then with poly(aniline)	LR = 3–9 pH unit; S = −51.2 mV $pH\ unit^{-1}$; RT ~ 0.5 s	Cerebrospinal fluid of rat brain	[99]
Dopamine / from 0 to +550 mV vs. Ag/AgCl, KCl (1 M)	Carbon fiber modified with a graphene and Fe tetrasulfophthalocyanine nanocomposite	DL = 50 nM; LR = (at least) 0.1–100 μM; S = 0.044 nA μM^{-1}	Striatum of mouse brain	[100]
5-Hydroxytryptamine / from 0 to +550 mV vs. Ag/AgCl, KCl (1 M)	Carbon fiber modified with a graphene and Fe tetrasulfophthalocyanine nanocomposite	DL = 20 nM; LR = (at least) 0.05–60 μM; S = 0.099 nA μM^{-1}	Striatum of mouse brain	[100]

materials used as 2D-films are most of the time included in sandwich-like composite structures without being directly exposed to cells/tissue/organ. Their role in such cases is restricted to amplify signals and/or reduce background noise and increase mechanical stability of the whole device. However, due to biodegradation, micro-nano fragments might reach secondary organs. Graphene has been proved to cross biological barriers, including gastro-intestinal, kidney and blood-brain (BBB) barriers [104]. Thus, biodegradation and full clearance of the materials from the body needs to be proved for biomedical applications. Finally, a last aspect to bear in mind is the possible chemical contamination of the materials already during their synthesis [103]. Potentially harmful chemicals should be replaced with more biocompatible alternatives and new protocols for cleaning/purification/sterilization of samples should be made available, including the production of endotoxin-free materials [106, 111, 112].

Biocompatibility of graphene and graphene based materials

Each 2D-material for biomedical application requires specific tests to assess its biocompatibility. For example, when using GBMs for drug delivery purposes, it is fundamental to test concentration-dependent cytotoxicity, to investigate the mechanisms of cytotoxicity in vitro and to probe the biodegradability of the material in vivo. On the other hand, when employing graphene scaffolds for tissue engineering purposes or when using graphene to build sensors for the investigation of biological systems, it is mandatory to monitor graphene mechanical stability, biocompatibility and long-term toxicity, to avoid the onset of chronic inflammation.

So far, graphene properties such as layer number (thickness), lateral dimension, surface chemistry and reactivity, agglomeration and presence of biomolecular corona have been identified as key parameters in determining graphene biocompatibility and have already been tested on different cell types [104, 105, 113, 114]. Interestingly, in case of sensors, surface properties (chemistry and reactivity) and topography seem to be crucial for GBMs biocompatibility [115]. For what concern the presence of contaminants produced during the synthesis process, nano-micro residues of poly(methylmethacrylate) (PMMA) typically used in the wet transfer of CVD graphene were seen to have pro-inflammatory and cytotoxic effects [116]. Recently, the issue was solved by dry-transfer protocols which exploit poly(vinyl alcohol) (PVA) rather than PMMA [117]. In case of rGO, the common reducing agent hydrazine, employed to obtain rGO from GO and well-known to be highly cytotoxic and carcinogenic [118], has been now substituted with L-ascorbic acid [119] or high temperature approaches [120], that will reduce GO without the possibility of introducing toxic contaminants. Electrochemical reduction was also demonstrated to be a simple and environmentally benign pathway to obtain graphene from rGO [121]. Similarly, mechanical and liquid phase graphite exfoliations to obtain graphene have already explored "green" solutions (e.g. melamine and glucose) to make GBMs suitable for biomedical applications [122, 123].

Interestingly, the biocompatibility of rGO (i.e. the biocompatibility of the GBM most often used in electrochemical sensors) is much less investigated than the biocompatibility of GO and pristine graphene [124]. However, given the concerns around the safety and biocompatibility of nanosheet suspensions, and speaking about electrochemical sensors, it is very unlikely that such devices will have nanosheet suspension design. Electrochemical sensors will be more likely implants for transient use, as for example intraoperative neural recording electrodes, where graphene attached to a substrate will

interface with brain surface for limited time [125]. Other target organs of toxicity might be the skin in case of wearable sensors and the blood and immune-system in case of sensors inserted into the circulatory system and degradation of the device and fragment release. In the latter case, second target organs might also be affected, such as lungs [126] and gastrointestinal tract [127], although with minor intensity and lower side effects.

Both pristine and functionalized graphene flakes were found to cause negligible haemolysis in red blood cells [128]. Not surprisingly, the smaller the lateral dimension of GO nanosheets is the longer the blood circulation time is, with an accumulation in the liver and residues in lungs and spleen. On the contrary, large GO nanosheets were observed to end up mainly in the lungs and small amount in the liver [129]. Of note, when their concentration is increased, small GO nanosheets accumulate in lungs too, indicating that a possible congestion of blood vessels due to GO agglomeration might occur in the capillary bed of the lungs. This agrees with a proven dose-dependent toxicity for graphene [130], which can be improved by surface functionalization.

As for other nanomaterials, functionalization of GBMs can in fact improve biocompatibility and stability of the materials in biological conditions. A good example of improved water-solubility and biocompatibility toward endothelial cells is the functionalization of rGO with a mussel inspired poly(dopamine) polymer [131]. Other widely and successfully used functionalization molecules are PVA, hydroxyethyl cellulose (HEC), poly(ethylene glycol) (PEG), poly(vinyl pyrrolidone), chondroitin, glucosamine, and hyaluronic acid [132]. Although all of them are able to dramatically reduce haemolysis, PVA and HEC seem to be the best choices to reach extremely valuable biocompatibility results, mainly due to a decrease in cellular uptake/internalization. In addition, PEG surface functionalization of few-layer graphene (FLG) showed a significant decrease of histological abnormalities in vivo compared to bare FLG [133]. On the other hand, non-functionalized GO nanosheets were seen to be excreted in the urine without damaging kidney and other tissues after intravenous injection [134]. Finally, if functionalized with poly(acrylic acid) or PEG, GO was noticed to acquire higher biocompatibility both in vitro and in vivo [135].

As mentioned above, the biocompatibility of GBMs depends both on the physical-chemical properties of the material and on the targeted biological system. Thus, in the following paragraphs we will briefly discuss the biocompatibility of GBMs in specific cell types/organ/tissues.

The very first barrier that any biomaterial or implant will face is the immune system. One of the first studies to address if macrophages, one of the main component of the immune system, are affected by GBMs compared the effect of GO of different sizes on human and murine primary macrophages [136]. The three GO materials tested displayed a dose-dependent cytotoxic effect, showing that the smaller the GO, the higher the internalization, leading to significant effects on cell viability and cell activation. Interestingly, another study based on two GO materials of different sizes showed opposite results, with no clear toxicity for both materials [137]. An interesting finding comes from the investigation of large GO that gets adsorbed onto cell membrane causing a "mask-effect" and, by interacting with Toll-like receptors, activate NF-kB pathway [138]. These effects were also confirmed in vivo, with the worst scenario provoked by large GO [138]. Recently it also became clear the importance of working with (not only sterile but also) endotoxin-free materials, especially when investigating immune effects. In this context, protocols to produce such materials have been published and the same materials tested versus human primary macrophages displayed no toxicity albeit GO and FLG cell internalization [112, 139]. Interestingly, what appears to be a common mechanism for many nanomaterials, including GBMs, is the activation of the inflammasome, that functions as an immuno-sensor for general exogenous agents [139, 140]. Once again, modification with PEG was shown to reduce the cytotoxic effects of GO on macrophages [141]. However, a recent report suggested that modification with PEG of small GO flakes resulted in the stimulation of a potent cytokine response, despite not being internalized by macrophages [142]. Finally, a recent study has shown that when they interact with isolated human neutrophils, another very important component of the immune system, GO sheets trigger a dose-dependent loss of cell viability and size-dependent formation of neutrophil extracellular traps (NETs) [143]. Overall, when comparing the results of different studies on GBMs, the toxicity of this class of materials toward macrophages, in particular, appears to be less pronounced as compared to the effects of carbon nanotubes [104].

Regarding the skin, a common biointerface for wearable sensors, the currently available literature is limited to one in vivo and a few in vitro studies, and it is not sufficient to draw any conclusion on the hazard related to dermal exposure to GBMs. The majority of studies are on skin keratinocytes and/or fibroblasts. Liao et al. evaluated the impact of a panel of different GOs and graphene sheets on skin fibroblasts, showing that, after 24 h exposure, graphene induces a cytotoxic effect higher than that of GO [144]. In more recent studies, the effect of GO and FLG were evaluated in immortalized human keratinocytes [145, 146]. Cytotoxic effect, which is dependent on the oxidative state of the GBMs, was observed. Moreover, mitochondrial dysfunction and plasma membrane disruption were noticed and associated with reactive oxygen species (ROS) induction [145]. The only in vivo study carried out presents the dermal effects of GO injected in the dermis of the growing feather sites of chickens to study local immune and inflammatory reaction [147]. The results displayed a certain ability of GO to initiate an immune response after dermal injection suggested by an increased infiltration of

lymphocytes and macrophages, raising some concern over GBM uses in contact with skin. Overall, the currently available literature is not sufficient to draw any conclusions on the hazard related to dermal exposure to GBMs.

Finally, sensors for neuronal recordings and biomolecule detection have gained more and more attention, especially since the discovery of electrical conductivity properties of graphene [148]. Recent works pointed the attention on the effect of chronic and acute exposure of GBMs on primary neurons [149, 150] and astrocytes [151–153] (Fig. 5a). Chronic graphene and GO exposure did not cause alterations in cell viability and network formation. However, a more detailed investigation on cell functionality revealed some pathophysiological effects specific to GO exposure at synaptic signaling level, indicating GO is able to interfere and alter neuronal post-synaptic currents, calcium oscillations and neuron-to-astrocyte communication [149, 151] (Fig. 5a). Mendonça and colleagues focused their studies on the BBB cell component, showing that BBB integrity was not affected after GBM treatment, while the functionalization with PEG, which is widely used in order to improve nanomaterial distribution and stability, led to a disruption of brain capillary endothelial cells (BCECs) monolayer composition, loss of cell structure and loss of cell-to-cell contact [156, 157]. All these findings point the attention on the biocompatibility of graphene nanosheets within the CNS in order to improve the design and engineering of graphene-based technologies for in vivo applications.

It is important to note that, for what concerns graphene-based scaffolds, in vitro studies demonstrated the viability of neuronal cells grown on planar substrates coated with GBMs, highlighting the ability of GBM films to promote neuronal growth and differentiation, and to stimulate neuronal activity [154, 158] (Fig. 5b). Moreover, previous works established that graphene films promote differentiation of human neural stem cells (hNSCs) toward neurons with respect to glia cells, compared to hNSCs grown on standard glass substrates [159]. CVD graphene films characterized by large lateral dimensions have been seen in general more biocompatible and safe than graphene nanosheets characterized by small lateral dimensions [160]. To obtain 2D graphene films, now also of large surface area, CVD on copper is the most common and used technique [161]. CVD graphene has now been widely explored as cellular interface since it promotes: *i.)* cardiomyogenic differentiation of mesenchymal stem cells without any sign of cytotoxicity [162], and *ii.)* neuronal and other mammalian cell growth and development [154, 158].

In summary, there have been conflicting reports in the literature with some suggesting that implanted GBMs are benign [163, 164] and others indicating adverse responses including cytotoxicity [149, 152, 165], inflammatory cell recruitment [165] and tissue fibrosis [166]. Overall, the field of GBM biocompatibility appears immature and in need of more systematic assessment of GBM potential side effects before any overarching conclusions can be made [103, 104].

Biocompatibility of non-graphene 2D materials

As mentioned in Section 3, TMDs are, after GBMs, the 2D materials most extensively investigated for the development of electrochemical sensors. According to the very few studies, TMDs exhibit relatively low toxicity and show improved biocompatibility when compared to GBMs [167]. The field of the TMD toxicity is in its infancy, thus further investigations have to be conducted in order to understand their health hazards, and compare the toxicity profiles of the different 2D materials. Among TMDs, MoS_2 is the most often studied for electrochemical sensing purposes followed by WS_2.

Several studies have explored the use of MoS_2 for sensing without addressing its effect on cell viability. On the other hand, the works that have investigated MoS_2 biocompatibility were performed with MoS_2 flakes while only few investigated the effects of MoS_2 films (which are used in the construction of electrochemical sensors).

A bio-absorbable MoS_2 based sensor for transient electronics has been developed to monitor the intracranial pressure, temperature, strain and motion of animals without displaying any side effect (Fig. 5c and d). The biocompatibility and biodegradability of the starting material (MoS_2 monolayer) and the products of dissolution (MoS_2 monolayer flakes) were demonstrated through long-term in vitro assays and in vivo evaluations [155]. Furthermore, Dou and collaborators designed a sensor for in situ monitoring the H_2O_2 secreted from live MCF-7 cancer cells that consisted of trimetallic hybrid nanoflowers-decorated MoS_2 nanosheets casted on disposable screen-printed carbon electrodes. The sensor showed limited cell adhesion capability when cells were seeded on the interface but the biocompatibility was significantly improved after further modifying the interface with laminin [77]. Unfortunately, the effect of the MoS_2 surface (without the nanoflowers) on cell adhesion was not assessed and the improved biocompatibility of the sensor was attributed to the laminin coating. Another recent study employed highly sensitive sensors, made with molybdenum-based 2D materials (MoO_3, MoS_2, and $MoSe_2$), to detect prostate specific antigen (PSA) through a fluorescence turn-on mechanism. In this case, the MoS_2 was not used as a scaffold (i.e. 2D film) but as flakes / nanosheets. While investigating the biocompatibility of the nanosheets, it was observed that about 80% of HEK 293 T cells taken into study survived even when the cells were incubated for 48 h with nanosheets in concentration as high as 100 μg mL^{-1} [168].

In the case of MoS_2 flakes, the effects of different physicochemical factors (such as the use of biomolecules as stabilizers during the exfoliation of the bulk material, the number of

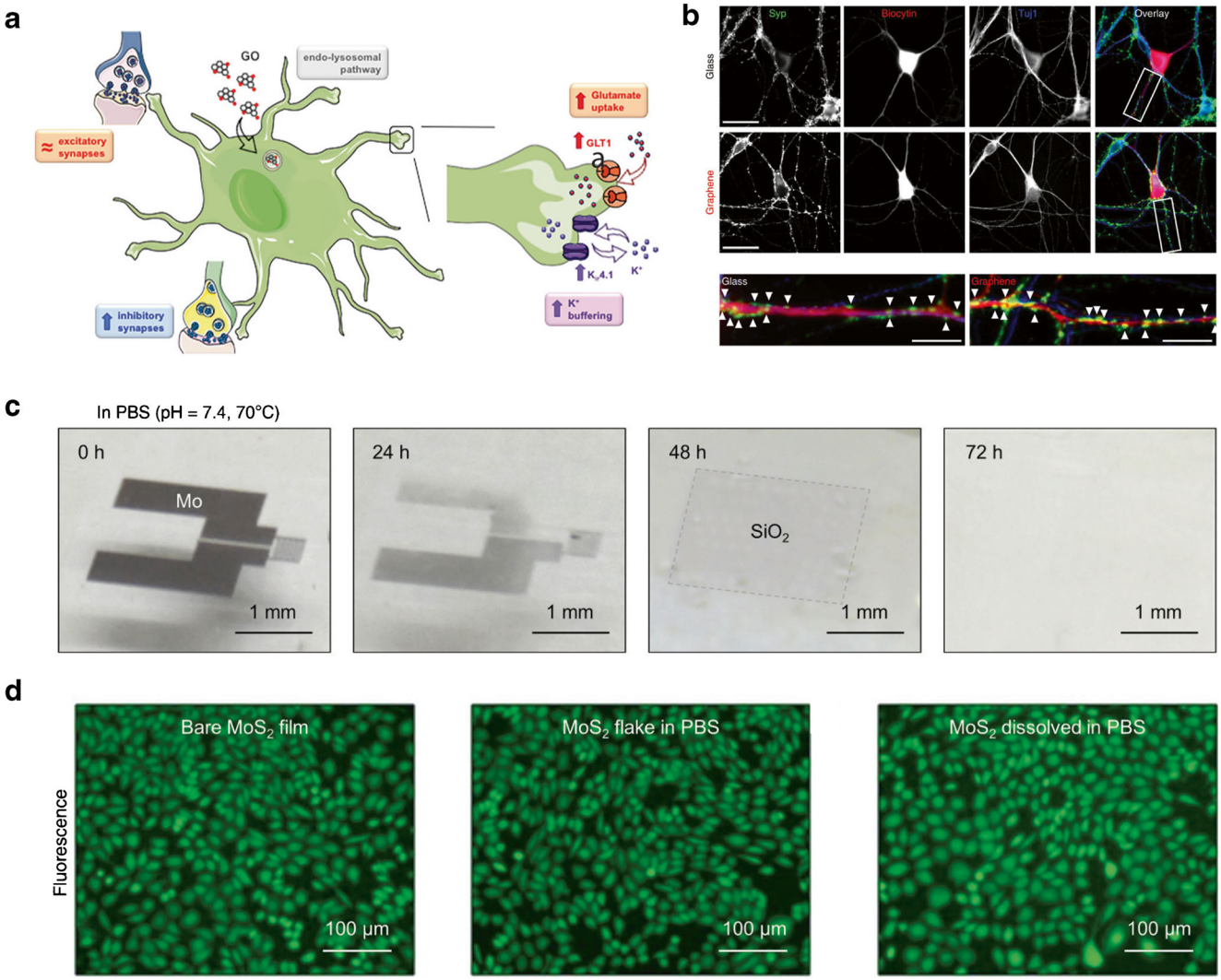

Fig. 5 Biocompatibility of GBMs and MoS_2; **(a)** Schematic cartoon depicting the biological effect of GO flakes on astrocytes and astrocyte-to-neuron cell communication. Reproduced with permission from Chiacchiaretta M, Bramini M, Rocchi A, Armirotti A, Giordano E, Vázquez E, Bandiera T, Ferroni S, Cesca F, Benfenati F. Graphene Oxide Upregulates the Homeostatic Functions of Primary Astrocytes and Modulates Astrocyte-to-Neuron Communication. Nano Lett. 2018;18:5827–5838. Copyright (2018) American Chemical Society. **(b)** Morphological comparison of neurons grown onto glass and CVD-graphene supports showing a comparable cellular development and, in the inset regions, a normal synaptic puncta expression. Reproduced with permission from [154]. **(c)** Optical images of a bioabsorbable sensor, consisting of a stack of SiO_2/Mo/MoS_2, in PBS solution (pH 7.4) at different dissolution times (from 0 to 72 h). **(d)** Fluorescence images of L-929 mouse fibroblast cells following 24 days of culture with different MoS_2 states, including MoS_2 continuous film, PBS with MoS_2 flakes, and dissolved MoS_2. Reproduced with permission from [155]

layers and the functionalization of the surface) on biocompatibility, has been assessed in recent years.

The use of functional biomolecules as stabilizers during the exfoliation of layered MoS_2 in aqueous solution has recently emerged demonstrating to improve the biocompatibility of the resulting MoS_2 flakes compared to synthetic stabilizers [169]. Indeed, Guan et al. demonstrated that bovine serum albumin (BSA) exfoliated MoS_2 flakes were much more biocompatible to fibroblast cells than bulk MoS_2 and flakes stabilized with polymers such as poly(acrylic acid) and poly(vinyl pyrrolidone) [170].

As for other layered 2D nanomaterials, the number of layers or thickness of MoS_2, has been demonstrated to affect biocompatibility [171, 172] although the findings are not concordant. It has been reported that the more exfoliated MoS_2 nanosheets are, the less biocompatible the material becomes, probably due to an increase in surface area and active edge sites. In particular, exfoliation performed with n-butyllithium and tert-butyllithium led to a decrease in the number of MoS_2 layers and a higher cytotoxic effect to A549 cells. Methyllithium provided a less efficient exfoliation and showed a toxicity profile largely similar to that of the bulk MoS_2 [172]. Contrary to this finding, a study of the pulmonary

hazard potential of three different MoS_2 based materials (MoS_2 exfoliated by lithiation, MoS_2 dispersed by Pluronic F87 and aggregated MoS_2) demonstrated that exfoliation attenuates the toxicity both in vitro (THP-1 monocytic and BEAS-2B bronchial epithelial cells) and in vivo (C57Bl/6 mouse model). Aggregated MoS_2 induced strong proinflammatory and profibrogenic response in vitro and acute lung inflammation in vivo, while MoS_2 flakes had little or no effect [171].

Finally, the functionalization of the surface of 2D MoS_2 induces significant changes in the physical-chemical properties of layered MoS_2 including surface charge and stability. This opens the way to control the toxicity profile of 2D TMD nanomaterials through surface functionalization [111]. Cytotoxicity assessment of MoS_2 flakes functionalized with different molecules (such as PEG and antibodies) for a variety of applications (e.g. photothermal therapy) has demonstrated the high biocompatibility of this 2D material [173–175]. Functionalization with PEG is one of the most commonly investigated and has demonstrated to improve the biocompatibility profile of MoS_2 flakes in vitro and in vivo. Liu and collaborators functionalized MoS_2 nanosheets with lipoic acid modified PEG to increase their biocompatibility. After 3 days of treatment, HeLa cells treated with plain MoS_2 flakes showed a slightly reduced viability (~80%) compared to cells treated with PEG-modified MoS_2 flakes which remained viable (over 90%) even at the highest concentration of PEG-modified MoS_2. Moreover, in vivo experiments showed that PEG-modified MoS_2 flakes were not toxic to mice models after 30 days of treatment [175].

It is important to note how only few works addressed the biocompatibility and biointeractions of bare MoS_2 nanosheets with living systems. A route for production of few-layered MoS_2 nanosheets in pure water has been reported. The MoS_2 nanosheets exhibited cytotoxic effects in tumor cells while normal cells were unaffected in the tested conditions [176]. The good biocompatibility of MoS_2 is also sustained by a study that investigated the effect of MoS_2 nanosheets on rat pheochromocytoma cells (PC12) and rat adrenal medulla endothelial cells (RAMEC) and found that the nanosheets are biocompatible up to 100 $\mu g\ mL^{-1}$ [177].

WS_2 is another TMD that has been exploited in the field of electrochemical sensors (see Section 3). Research on WS_2 nanosheets has shown good biocompatibility for both naked [178] and functionalized flakes [179]. Very recently, the capacity of WS_2 nanosheets (and few other TMDs such as WSe_2, MoS_2, $MoSe_2$) to inhibit oxidative stress in living cells and their great biocompatibility has been demonstrated. First, nanosheets were functionalized with poly(ε-caprolactone)-b-poly (ethylene oxide) copolymer (PCL-b-PEG) during in situ exfoliation and then, tested against a human keratinocyte cell line (HaCaT cells) showing excellent scavenging activity for ROS and biocompatibility. In a more recent study, WS_2 functionalized with PCL-b-PEG were embedded within hydrogel systems improving the cell viability of a mouse fibroblast cell line (L929 cells), and of human HaCaT cells thanks to their ROS scavenging capabilities [179].

MXenes have also been used to construct sensors (see Section 3) but the biocompatibility of these 2D materials has been largely unexplored to date. A recent investigation showed in vitro cytotoxicity of 2D sheets of Ti_3C_2 MXene. The observed toxic effects were higher against cancerous cells compared to normal ones at extremely high concentrations (from 125 to 500 $\mu g\ mL^{-1}$). Authors suggest that these differences might be due to differences in the morphology and permeability of normal and cancerous cells. Nevertheless, at the lowest MXene concentration tested (62.5 $\mu g\ mL^{-1}$, a concentration that is still quite high compared to typical concentrations used in nanotoxicology studies) about 80–90% of cells survived. ROS generation was proposed as the possible mechanism of cytotoxicity of Ti_3C_2 [180]. The biocompatibility of 2D Ti_3C_2 sheets (as part of a nanoplatform, containing also GOx and superparamagnetic iron oxide nanoparticles, for treatment of tumors through hyperthermia) was also demonstrated in vivo [181]. Finally, other studies have explored the biocompatibility profile of 2D Ti_3C_2 MXene as part of composites with different applications such as regenerative therapies [182], high resolution neural interfaces [183] and bioregeneration [184]. In these cases, the material was used as a support to grow cells and 2D Ti_3C_2 has shown to be biocompatible sustaining cell adhesion and viability.

Biodegradation of 2D materials

In the last decade, there has been an increased number of studies addressing biodegradability and biodistribution of GBMs. These studies show that, although carbon-based material were thought to be persistent, GBMs can actually be degraded by oxidative enzymes [185–187] and be naturally cleared by the body [134]. Among GBMs, GO is the most studied and it was seen to be faster degraded in artificial acidic fluid of hypochlorite than nanohorns and single-wall oxidized carbon nanotubes [188]. Interestingly, PEG and BSA protect GO from degradation by HRP [189]. On the other hand, to make the material biodegradable, one can functionalize GO with coumarin and catechol, two natural substrates of HRP [190]. Recently, the degradation of single-layer graphene and FLG has also been demonstrated by human myeloperoxidase (MPO) and in presence of human neutrophils [187].

For what concerns other 2D materials such as TMDs, there is a big gap in the investigation of their biodegradation. One study on this subject showed that poly(vinyl pyrrolidone)-modified MoS_2 nanosheets exhibit different biodegradability levels in bio-microenvironments with H_2O_2, catalase and human myeloperoxidase (H_2O_2 > catalase > hMPO, at physiological concentrations) implying that this 2D material can be degraded in the liver and spleen [191].

Conclusions

Living cells release tiny amounts of chemicals into their extracellular space. The released chemicals are rapidly taken up by other cells, they get converted by (bio)chemical reactions, or simply diffuse away and get very much diluted. As a consequence, the released chemicals persist in the extracellular space, in detectable concentrations, for a limited time only. Electrochemical sensors are among the very few analytical tools which are characterized by appropriate sensitivity and response time to allow monitoring the dynamics of these processes. Since the discovery of graphene in 2004, such sensors are increasingly enhanced through the use of 2D materials. Therefore, we set out to review electrochemical sensors made with 2D materials and used to investigate living cells. rGO (rather than graphene) was discovered to be the 2D material most often used to enhance electrochemical sensors for investigating living cells. MoS_2 is also a popular choice when it comes to improving such sensors. The direct comparison of the different 2D materials, as building blocks for electrochemical sensors suitable to investigate cells, was very seldom carried out. One study shows that electrochemical sensors for the detection of H_2O_2, made with MoS_2 nanosheets and PtW nanocubes, are characterized by better selectivity and better sensitivity than similar sensors in which MoS_2 was replaced with either graphene or WS_2 [73]. Another study points out that electrochemical H_2O_2 sensors made with $Mo_{0.75}W_{0.25}S_2$ are characterized by higher sensitivity than H_2O_2 sensors made in a similar manner but with either MoS_2 or WS_2 [83]. Additional work is needed in order to identify the exact advantages each 2D material is providing for electrochemical sensors and to identify which 2D material suits better the detection of a certain analyte in living systems. Such studies would help the community focus on the right 2D material. H_2O_2 and ·NO are the small molecules of which cellular release was most often monitored using the electrochemical sensors made with 2D materials. When used not at cell culture level but as wearable sensors (placed onto the skin or the eyeball as mentioned in Section 4), electrochemical sensors are made most often with GBMs, target glucose, and, thus, promise to improve the way diabetes is managed. Electrochemical sensors made with 2D materials to be used in vivo are most often fabricated with GBMs and target dopamine. In this case, the use of GBMs increases the sensitivity of such sensors for this important neurotransmitter.

Electrochemical sensors made with 2D materials and used to investigate living cells have also some weaknesses important to mention: *1.)* Very often 2D materials play only a secondary role in these electrochemical sensors. In yet other words, 2D materials are very often replaceable support for more traditional electrocatalysts such as noble metal nanoparticles. The synergy in between the 2D material and the more traditional electrocatalyst is often claimed but seldom proved without leaving room for doubt; *2.)* Unfortunately, the use of 2D materials did not facilitate detecting new compounds of interest. Electrochemical sensors made with 2D materials detect the very same species as sensors previously developed without 2D materials; *3.)* While much effort was put into making the electrochemical sensors the problem of placing the sensors to known and controlled distances from cells was very seldom solved; *4.)* Selectivity tests are often carried out using wrong concentrations of analyte and of possibly interfering compounds; *5.)* The number of experiments carried out at cellular level with the developed electrochemical sensors is most often very low. Suitability of the electrochemical sensors for the investigation of living cells must be more convincingly proved with a higher number of experiments carried out at cellular level.

The extent to which electrochemical sensors made with 2D materials will be used at cellular level, as wearable sensors, or as sensors for in vivo measurements depends also on the biocompatibility of the 2D materials. The unique properties of graphene and non-graphene 2D materials open a completely new scenario in the nanotoxicology research, making the old approaches commonly used to assess nanomaterial and biomaterial toxicity not any more reliable and sufficient. The general conclusion about 2D material toxicity is that they can be categorized according to physical-chemical characteristics and cannot be considered as a single type of material. Analysis of the literature on this topic (see Section 5) showed that, depending on the form of the 2D material (i.e. on the number of layers, lateral dimension, surface chemistry, exposure time, concentration, etc.) and the used biological model, 2D materials can be both harmful and biocompatible. When trying to translate the use of graphene and non-graphene 2D materials into medicine, researchers can follow some already available suggestions: *1.)* Characterize and design the material in line with a safe approach and with respect to the structure–activity relationship; *2.)* Avoid chemical contamination and think about "green" and biocompatible alternative products; and *3.)* Consider a sterilization strategy that is compatible with all sensor components.

The importance of combining sensor development efforts with biocompatibility studies is obviously increasing when the electrochemical sensors are meant to be in contact with the investigated tissue for prolonged times (e.g. in the case of wearable sensors and sensors to be used in vivo). It is also important that proof-of-principle studies are followed by in depth studies on the performance of the electrochemical sensors made with 2D materials in real-life conditions. Such follow-up studies are currently very much missing. The lack of detailed biocompatibility and follow-up studies suggests that the integration of electrochemical sensors made with 2D materials into a commercially viable device is still years away.

Acknowledgements Financial support from the Romanian Executive Agency for Higher Education, Research, Development and Innovation Funding (through the EuroNanoMed III project nanoLight, Grant Agreement No. 135 from 09/03/2020) and from the European Union's Horizon 2020 research and innovation program through the MSCA-COFUND Athenea3i scheme (Grant Agreement No. 754446) is gratefully acknowledged.

Compliance with ethical standards

Conflict of interest The authors declare that they have no conflict of interest.

References

1. Bucher ES, Wightman RM. Electrochemical analysis of neurotransmitters. Annu Rev Anal Chem. 2015;8:239–61.
2. Lulevich V, Shih Y-P, Lo SH, Liu G. Cell tracing dyes significantly change single cell mechanics. J Phys Chem B. 2009;113(18):6511–9.
3. Hu K, Liu Y-L, Oleinick A, Mirkin MV, Huang W-H, Amatore C. Nanoelectrodes for intracellular measurements of reactive oxygen and nitrogen species in single living cells. Curr Opin Electrochem. 2020;22:44–50.
4. Chen A, Chatterjee S. Nanomaterials based electrochemical sensors for biomedical applications. Chem Soc Rev. 2013;42:5425–38.
5. Novoselov KS, Geim AK, Morozov SV, Jiang D, Zhang Y, Dubonos SV, et al. Electric field effect in atomically thin carbon films. Science. 2004;306(5696):666–9.
6. Wu S, He Q, Tan C, Wang Y, Zhang H. Graphene-based electrochemical sensors. Small. 2013;9(8):1160–72.
7. Yin PT, Kim T-H, Choi J-W, Lee K-B. Prospects for graphene–nanoparticle-based hybrid sensors. Phys Chem Chem Phys. 2013;15:12785–99.
8. Zhu C, Dong S. Energetic graphene-based electrochemical analytical devices in nucleic acid, protein and cancer diagnostics and detection. Electroanalysis. 2014;26(1):14–29.
9. Zhu C, Du D, Lin Y. Graphene-like 2D nanomaterial-based biointerfaces for biosensing applications. Biosens Bioelectron. 2017;89:43–55.
10. Meng Z, Stolz RM, Mendecki L, Mirica KA. Electrically-transduced chemical sensors based on two-dimensional nanomaterials. Chem Rev. 2019;119(1):478–598.
11. Kalambate PK, Gadhari NS, Li X, Rao Z, Navale ST, Shen Y, et al. Recent advances in MXene–based electrochemical sensors and biosensors. TrAC Trends Anal Chem. 2019;120:115643.
12. Mazánek V, Luxa J, Matějková S, Kučera J, Sedmidubský D, Pumera M, et al. Ultrapure graphene is a poor electrocatalyst: definitive proof of the key role of metallic impurities in graphene-based electrocatalysis. ACS Nano. 2019;13(2):1574–82.
13. Zhang T, Gu Y, Li C, Yan X, Lu N, Liu H, et al. Fabrication of novel electrochemical biosensor based on graphene nanohybrid to detect H_2O_2 released from living cells with ultrahigh performance. ACS Appl Mater Interfaces. 2017;9(43):37991–9.
14. Yang G-H, Zhou Y-H, Wu J-J, Cao J-T, Li L-L, Liu H-Y, et al. Microwave-assisted synthesis of nitrogen and boron co-doped graphene and its application for enhanced electrochemical detection of hydrogen peroxide. RSC Adv. 2013;3(44):22597–604.
15. Xiao F, Li Y, Zan X, Liao K, Xu R, Duan H. Growth of metal–metal oxide nanostructures on freestanding graphene paper for flexible biosensors. Adv Funct Mater. 2012;22(12):2487–94.
16. Li X-R, Kong F-Y, Liu J, Liang T-M, Xu J-J, Chen H-Y. Synthesis of potassium-modified graphene and its application in nitrite-selective sensing. Adv Funct Mater. 2012;22(9):1981–8.
17. Bai J, Jiang X. A facile one-pot synthesis of copper sulfide-decorated reduced graphene oxide composites for enhanced detecting of H_2O_2 in biological environments. Anal Chem. 2013;85(17):8095–101.
18. Xi F, Zhao D, Wang X, Chen P. Non-enzymatic detection of hydrogen peroxide using a functionalized three-dimensional graphene electrode. Electrochem Commun. 2013;26:81–4.
19. Ting SL, Guo CX, Leong KC, Kim D-H, Li CM, Chen P. Gold nanoparticles decorated reduced graphene oxide for detecting the presence and cellular release of nitric oxide. Electrochim Acta. 2013;111:441–6.
20. Zhang Y, Bai X, Wang X, Shiu K-K, Zhu Y, Jiang H. Highly sensitive graphene–Pt nanocomposites amperometric biosensor and its application in living cell H_2O_2 detection. Anal Chem. 2014;86(19):9459–65.
21. Fang H, Pan Y, Shan W, Guo M, Nie Z, Huang Y, et al. Enhanced nonenzymatic sensing of hydrogen peroxide released from living cells based on Fe_3O_4 /self-reduced graphene nanocomposites. Anal Methods. 2014;6:6073–81.
22. Maji SK, Sreejith S, Mandal AK, Ma X, Zhao Y. Immobilizing gold nanoparticles in mesoporous silica covered reduced graphene oxide: a hybrid material for cancer cell detection through hydrogen peroxide sensing. ACS Appl Mater Interfaces. 2014;6(16):13648–56.
23. Hu FX, Xie JL, Bao SJ, Yu L, Li CM. Shape-controlled ceria-reduced graphene oxide nanocomposites toward high-sensitive in situ detection of nitric oxide. Biosens Bioelectron. 2015;70:310–7.
24. Li J, Xie J, Gao L, Li CM. Au nanoparticles–3D graphene hydrogel nanocomposite to boost synergistically in situ detection sensitivity toward cell-released nitric oxide. ACS Appl Mater Interfaces. 2015;7(4):2726–34.
25. Liu J, Bo X, Zhao Z, Guo L. Highly exposed Pt nanoparticles supported on porous graphene for electrochemical detection of hydrogen peroxide in living cells. Biosens Bioelectron. 2015;74:71–7.
26. Liu Y-L, Wang X-Y, Xu J-Q, Xiao C, Liu Y-H, Zhang X-W, et al. Functionalized graphene-based biomimetic microsensor interfacing with living cells to sensitively monitor nitric oxide release. Chem Sci. 2015;6:1853–8.
27. Sun Y, He K, Zhang Z, Zhou A, Duan H. Real-time electrochemical detection of hydrogen peroxide secretion in live cells by Pt nanoparticles decorated graphene–carbon nanotube hybrid paper electrode. Biosens Bioelectron. 2015;68:358–64.
28. Yu G, Wu W, Pan X, Zhao Q, Wei X, Lu Q. High sensitive and selective sensing of hydrogen peroxide released from pheochromocytoma cells based on Pt-Au bimetallic nanoparticles electrodeposited on reduced graphene sheets. Sensors. 2015;15(2):2709–22.
29. Wang L, Zhang Y, Cheng C, Liu X, Jiang H, Wang X. Highly sensitive electrochemical biosensor for evaluation of oxidative stress based on the nanointerface of graphene nanocomposites blended with Au, Fe_3O_4 and Pt nanoparticles. ACS Appl Mater Interfaces. 2015;7(33):18441–9.
30. Abdurhman AAM, Zhang Y, Zhang G, Wang S. Hierarchical nanostructured noble metal/metal oxide/graphene-coated carbon fiber: in situ electrochemical synthesis and use as microelectrode for real-time molecular detection of cancer cells. Anal Bioanal Chem. 2015;407:8129–36.
31. Yu C, Wang L, Li W, Zhu C, Bao N, Gu H. Detection of cellular H_2O_2 in living cells based on horseradish peroxidase at the interface of Au nanoparticles decorated graphene oxide. Sensors Actuators B Chem. 2015;211:17–24.
32. Liu Z, Forsyth H, Khaper N, Chen A. Sensitive electrochemical detection of nitric oxide based on AuPt and reduced graphene oxide nanocomposites. Analyst. 2016;141(13):4074–83.
33. Bai Z, Li G, Liang J, Su J, Zhang Y, Chen H, et al. Non-enzymatic electrochemical biosensor based on Pt NPs/RGO-CS-Fc nanohybrids for the detection of hydrogen peroxide in living cells. Biosens Bioelectron. 2016;82:185–94.

34. Li C, Liu X, Zhang Y, Chen Y, Du T, Jiang H, et al. A novel nonenzymatic biosensor for evaluation of oxidative stress based on nanocomposites of graphene blended with CuI. Anal Chim Acta. 2016;933:66–74.
35. Suhag D, Sharma AK, Patni P, Garg SK, Rajput SK, Chakrabarti S, et al. Hydrothermally functionalized biocompatible nitrogen doped graphene nanosheet based biomimetic platforms for nitric oxide detection. J Mater Chem B. 2016;4(27):4780–9.
36. Zhang D, Ouyang X, Li L, Dai B, Zhang Y. Real-time amperometric monitoring of cellular hydrogen peroxide based on electrodeposited reduced graphene oxide incorporating adsorption of electroactive methylene blue hybrid composites. J Electroanal Chem. 2016;780:60–7.
37. Zhang Y, Xiao J, Lv Q, Wang L, Dong X, Asif M, et al. In situ electrochemical sensing and real-time monitoring live cells based on freestanding nanohybrid paper electrode assembled from 3D functionalized graphene framework. ACS Appl Mater Interfaces. 2017;9(44):38201–10.
38. Tian Y, Wei Z, Zhang K, Peng S, Zhang X, Liu W, et al. Three-dimensional phosphorus-doped graphene as an efficient metal-free electrocatalyst for electrochemical sensing. Sensors Actuators B Chem. 2017;241:584–91.
39. Liu Y, Liu X, Guo Z, Hu Z, Xue Z, Lu X. Horseradish peroxidase supported on porous graphene as a novel sensing platform for detection of hydrogen peroxide in living cells sensitively. Biosens Bioelectron. 2017;87:101–7.
40. Sun Y, Luo M, Meng X, Xiang J, Wang L, Ren Q, et al. Graphene/intermetallic PtPb nanoplates composites for boosting electrochemical detection of H_2O_2 released from cells. Anal Chem. 2017;89(6):3761–7.
41. Sun Y, Luo M, Qin Y, Zhu S, Li Y, Xu N, et al. Atomic-thick PtNi nanowires assembled on graphene for high-sensitivity extracellular hydrogen peroxide sensors. ACS Appl Mater Interfaces. 2017;9(40):34715–21.
42. Zhao Y, Huo D, Bao J, Yang M, Chen M, Hou J, et al. Biosensor based on 3D graphene-supported Fe_3O_4 quantum dots as biomimetic enzyme for in situ detection of H_2O_2 released from living cells. Sensors Actuators B Chem. 2017;244:1037–44.
43. Fu Y, Huang D, Li C, Zou L, Ye B. Graphene blended with SnO_2 and Pd-Pt nanocages for sensitive non-enzymatic electrochemical detection of H_2O_2 released from living cells. Anal Chim Acta. 2018;1014:10–8.
44. Wang Y, Wang M-Q, Lei L-L, Chen Z-Y, Liu Y-S, Bao S-J. $FePO_4$ embedded in nanofibers consisting of amorphous carbon and reduced graphene oxide as an enzyme mimetic for monitoring superoxide anions released by living cells. Microchim Acta. 2018;185:140.
45. Xu H, Liao C, Liu Y, Ye B-C, Liu B. Iron phthalocyanine decorated nitrogen-doped graphene biosensing platform for real-time detection of nitric oxide released from living cells. Anal Chem. 2018;90(7):4438–44.
46. Dong W, Ren Y, Bai Z, Yang Y, Wang Z, Zhang C, et al. Trimetallic AuPtPd nanocomposites platform on graphene: applied to electrochemical detection and breast cancer diagnosis. Talanta. 2018;189:79–85.
47. Munteanu R-E, Stănică L, Gheorghiu M, Gáspár S. Measurement of the extracellular pH of adherently growing mammalian cells with high spatial resolution using a voltammetric pH microsensor. Anal Chem. 2018;90(11):6899–905.
48. Liu Y, Shang T, Liu Y, Liu X, Xue Z, Liu X. Highly sensitive platinum nanoparticles-embedded porous graphene sensor for monitoring ROS from living cells upon oxidative stress. Sensors Actuators B Chem. 2018;263:543–9.
49. Dou B, Li J, Jiang B, Yuan R, Xiang Y. DNA-templated in situ synthesis of highly dispersed AuNPs on nitrogen-doped graphene for real-time electrochemical monitoring of nitric oxide released from live cancer cells. Anal Chem. 2019;91(3):2273–8.
50. Bai W-S, Zhang X-J, Zheng J-B. Direct growth of ordered PdCu and Co doped PdCu nanoparticles on graphene oxide based on a one-step hydrothermal method for ultrasensitive sensing of H_2O_2 in living cells. Analyst. 2019;144(1):157–60.
51. Dong W, Ren Y, Bai Z, Yang Y, Chen Q. Fabrication of hexahedral Au-Pd/graphene nanocomposites biosensor and its application in cancer cell H_2O_2 detection. Bioelectrochemistry. 2019;128:274–82.
52. Wang W, Tang H, Wu Y, Zhang Y, Li Z. Highly electrocatalytic biosensor based on hemin@AuNPs/reduced graphene oxide/chitosan nanohybrids for non-enzymatic ultrasensitive detection of hydrogen peroxide in living cells. Biosens Bioelectron. 2019;132:217–23.
53. Li Y-T, Jin X, Tang L, Lv W-L, Xiao M-M, Zhang Z-Y, et al. Receptor-mediated field effect transistor biosensor for real-time monitoring of glutamate release from primary hippocampal neurons. Anal Chem. 2019;91(13):8229–36.
54. Qi H, Song J, Fu Y, Wu X, Qi H. Highly dispersive Pt–Pd nanoparticles on graphene oxide sheathed carbon fiber microelectrodes for electrochemical detection of H_2O_2 released from living cells. Nanotechnology. 2020;31(13):135503.
55. Veal EA, Day AM, Morgan BA. Hydrogen peroxide sensing and signaling. Mol Cell. 2007;26(1):1–14.
56. Dhalla NS, Temsah RM, Netticadan T. Role of oxidative stress in cardiovascular diseases. J Hypertens. 2000;18(6):655–73.
57. Dias V, Junn E, Mouradian MM. The role of oxidative stress in Parkinson's disease. J Parkinsons Dis. 2013;3(4):461–91.
58. Sultana R, Butterfield DA. Role of oxidative stress in the progression of Alzheimer's disease. J Alzheimers Dis. 2010;19(1):341–53.
59. Harrison D, Griendling KK, Landmesser U, Hornig B, Drexler H. Role of oxidative stress in atherosclerosis. Am J Cardiol. 2003;91(3A):7A–11A.
60. Klaunig JE, Kamendulis LM. The role of oxidative stress in carcinogenesis. Annu Rev Pharmacol Toxicol. 2004;44:239–67.
61. Butler AR, Williams DLH. The physiological role of nitric oxide. Chem Soc Rev. 1993;22(4):233–41.
62. Fukumura D, Kashiwagi S, Jain RK. The role of nitric oxide in tumour progression. Nat Rev Cancer. 2006;6(7):521–34.
63. Clancy RM, Amin AR, Abramson SB. The role of nitric oxide in inflammation and immunity. Arthritis Rheum. 1998;41(7):1141–51.
64. Kong X-K, Chen C-L, Chen Q-W. Doped graphene for metal-free catalysis. Chem Soc Rev. 2014;43(8):2841–57.
65. Sies H. Hydrogen peroxide as a central redox signaling molecule in physiological oxidative stress: oxidative eustress. Redox Biol. 2017;11:613–9.
66. Hall CN, Garthwaite J. What is the real physiological NO concentration *in vivo*? Nitric Oxide. 2009;21(2):92–103.
67. Niu N, Wang L. *In vitro* human cell line models to predict clinical response to anticancer drugs. Pharmacogenomics. 2015;16(3):273–85.
68. Katt ME, Placone AL, Wong AD, Xu ZS, Searson PC. *In vitro* tumor models: advantages, disadvantages, variables, and selecting the right platform. Front Bioeng Biotechnol. 2016;4:12.
69. Fitzmaurice C, Dicker D, Pain A, Hamavid H, Moradi-Lakeh M, MacIntyre MF, et al. The global burden of cancer 2013. JAMA Oncol. 2015;1(4):505–27.
70. Lennicke C, Rahn J, Lichtenfels R, Wessjohann LA, Seliger B. Hydrogen peroxide – production, fate and role in redox signaling of tumor cells. Cell Commun Signal CCS. 2015;13:39.
71. Wang T, Zhu H, Zhuo J, Zhu Z, Papakonstantinou P, Lubarsky G, et al. Biosensor based on ultrasmall MoS_2 nanoparticles for

electrochemical detection of H_2O_2 released by cells at the nanomolar level. Anal Chem. 2013;85(21):10289–95.
72. Tang J, Quan Y, Zhang Y, Jiang M, Al-Enizi AM, Kong B, et al. Three-dimensional WS_2 nanosheet networks for H_2O_2 produced for cell signaling. Nanoscale. 2016;8(10):5786–92.
73. Zhu L, Zhang Y, Xu P, Wen W, Li X, Xu J. PtW/MoS_2 hybrid nanocomposite for electrochemical sensing of H_2O_2 released from living cells. Biosens Bioelectron. 2016;80:601–6.
74. Shu Y, Chen J, Xu Q, Wei Z, Liu F, Lu R, et al. MoS_2 nanosheet-Au nanorod hybrids for highly sensitive amperometric detection of H_2O_2 in living cells. J Mater Chem B. 2017;5(7):1446–53.
75. Shu Y, Xu J, Chen J, Xu Q, Xiao X, Jin D, et al. Ultrasensitive electrochemical detection of H_2O_2 in living cells based on ultrathin MnO_2 nanosheets. Sensors Actuators B Chem. 2017;252:72–8.
76. Zhou J-X, Tang L-N, Yang F, Liang F-X, Wang H, Li Y-T, et al. MoS_2/Pt nanocomposite-functionalized microneedle for real-time monitoring of hydrogen peroxide release from living cells. Analyst. 2017;142(22):4322–9.
77. Dou B, Yang J, Yuan R, Xiang Y. Trimetallic hybrid nanoflower-decorated MoS_2 nanosheet sensor for direct in situ monitoring of H_2O_2 secreted from live cancer cells. Anal Chem. 2018;90(9):5945–50.
78. Dai H, Chen D, Cao P, Li Y, Wang N, Sun S, et al. Molybdenum sulfide/nitrogen-doped carbon nanowire-based electrochemical sensor for hydrogen peroxide in living cells. Sensors Actuators B Chem. 2018;276:65–71.
79. Du H, Zhang X, Liu Z, Qu F. A supersensitive biosensor based on MoS_2 nanosheet arrays for the real-time detection of H_2O_2 secreted from living cells. Chem Commun. 2019;55(65):9653–6.
80. Mani V, Shanthi S, Peng T-K, Lin H-Y, Ikeda H, Hayakawa Y, et al. Real-time quantification of hydrogen peroxide production in living cells using $NiCo_2S_4$@CoS_2 heterostructure. Sensors Actuators B Chem. 2019;287:124–30.
81. Zheng J, Wang B, Jin Y, Weng B, Chen J. Nanostructured MXene-based biomimetic enzymes for amperometric detection of superoxide anions from HepG2 cells. Microchim Acta. 2019;186:95.
82. Lu J, Hu Y, Wang P, Liu P, Chen Z, Sun D. Electrochemical biosensor based on gold nanoflowers-encapsulated magnetic metal-organic framework nanozymes for drug evaluation with in-situ monitoring of H_2O_2 released from H9C2 cardiac cells. Sensors Actuators B Chem. 2020;311:127909.
83. Shu Y, Zhang W, Yin X, Zhang L, Yang Y, Ma D, et al. Efficient electrochemical biosensing of hydrogen peroxide on bimetallic $Mo_{1-x}W_xS_2$ nanoflowers. J Colloid Interface Sci. 2020;566:248–56.
84. Shu Y, Zhang L, Cai H, Yang Y, Zeng J, Ma D, et al. Hierarchical Mo_2C@MoS_2 nanorods as electrochemical sensors for highly sensitive detection of hydrogen peroxide and cancer cells. Sensors Actuators B Chem. 2020;311:127863.
85. Vilian ATE, Dinesh B, Kang S-M, Krishnan UM, Huh YS, Han Y-K. Recent advances in molybdenum disulfide-based electrode materials for electroanalytical applications. Microchim Acta. 2019;186:203.
86. Mannoor MS, Tao H, Clayton JD, Sengupta A, Kaplan DL, Naik RR, et al. Graphene-based wireless bacteria detection on tooth enamel. Nat Commun. 2012;3:763.
87. Lee H, Choi TK, Lee YB, Cho HR, Ghaffari R, Wang L, et al. A graphene-based electrochemical device with thermoresponsive microneedles for diabetes monitoring and therapy. Nat Nanotechnol. 2016;11:566–72.
88. Kim J, Kim M, Lee M-S, Kim K, Ji S, Kim Y-T, et al. Wearable smart sensor systems integrated on soft contact lenses for wireless ocular diagnostics. Nat Commun. 2017;8:14997.
89. Lee H, Song C, Hong YS, Kim MS, Cho HR, Kang T, et al. Wearable/disposable sweat-based glucose monitoring device with multistage transdermal drug delivery module. Sci Adv. 2017;3:e1601314.
90. Lipani L, Dupont BGR, Doungmene F, Marken F, Tyrrell RM, Guy RH, et al. Non-invasive, transdermal, path-selective and specific glucose monitoring via a graphene-based platform. Nat Nanotechnol. 2018;13:504–11.
91. Park J, Kim J, Kim S-Y, Cheong WH, Jang J, Park Y-G, et al. Soft, smart contact lenses with integrations of wireless circuits, glucose sensors, and displays. Sci Adv. 2018;4:eaap9841.
92. Xuan X, Yoon HS, Park JY. A wearable electrochemical glucose sensor based on simple and low-cost fabrication supported micropatterned reduced graphene oxide nanocomposite electrode on flexible substrate. Biosens Bioelectron. 2018;109:75–82.
93. Jin Q, Chen H-J, Li X, Huang X, Wu Q, He G, et al. Reduced graphene oxide nanohybrid-assembled microneedles as minimally invasive electrodes for real-time transdermal biosensing. Small. 2019;15(6):1804298.
94. Toi PT, Trung TQ, Dang TML, Bae CW, Lee N-E. Highly electrocatalytic, durable, and stretchable nanohybrid fiber for on-body sweat glucose detection. ACS Appl Mater Interfaces. 2019;11(11):10707–17.
95. Klonoff DC. Continuous glucose monitoring: roadmap for 21st century diabetes therapy. Diabetes Care. 2005;28(5):1231–9.
96. Taylor IM, Robbins EM, Catt KA, Cody PA, Happe CL, Cui XT. Enhanced dopamine detection sensitivity by PEDOT/graphene oxide coating on *in vivo* carbon fiber electrodes. Biosens Bioelectron. 2017;89:400–10.
97. Pu Z, Tu J, Han R, Zhang X, Wu J, Fang C, et al. A flexible enzyme-electrode sensor with cylindrical working electrode modified with a 3D nanostructure for implantable continuous glucose monitoring. Lab Chip. 2018;18(23):3570–7.
98. Zhang B, Li C, Zhang H, Chen Y, Jiang H, Chen L, et al. *In Vivo* dopamine biosensor based on copper(I) sulfide functionalized reduced graphene oxide decorated microelectrodes. J Biomed Nanotechnol. 2018;14(7):1277–86.
99. Zhou J-X, Ding F, Tang L-N, Li T, Li Y-H, Zhang Y-J, et al. Monitoring of pH changes in a live rat brain with MoS_2/PAN functionalized microneedles. Analyst. 2018;143(18):4469–75.
100. Zhu M, Zeng C, Ye J, Sun Y. Simultaneous *in vivo* voltammetric determination of dopamine and 5-hydroxytryptamine in the mouse brain. Appl Surf Sci. 2018;455:646–52.
101. Chinta SJ, Andersen JK. Dopaminergic neurons. Int J Biochem Cell Biol. 2005;37(5):942–6.
102. Gonon F, Cespuglio R, Ponchon JL, Buda M, Jouvet M, Adams RN, et al. *In vivo* continuous electrochemical determination of dopamine release in rat neostriatum. C R Hebd Seances Acad Sci Ser Sci Nat. 1978;286(16):1203–6.
103. Bullock CJ, Bussy C. Biocompatibility considerations in the design of graphene biomedical materials. Adv Mater Interfaces. 2019;6:1900229.
104. Fadeel B, Bussy C, Merino S, Vázquez E, Flahaut E, Mouchet F, et al. Safety assessment of graphene-based materials: focus on human health and the environment. ACS Nano. 2018;12(11):10582–620.
105. Martín C, Kostarelos K, Prato M, Bianco A. Biocompatibility and biodegradability of 2D materials: graphene and beyond. Chem Commun. 2019;55(39):5540–6.
106. Wang S, Yang X, Zhou L, Li J, Chen H. 2D nanostructures beyond graphene: preparation, biocompatibility and biodegradation behaviors. J Mater Chem B. 2020;8(15):2974–89.
107. Reina G, Gonzalez-Dominguez JM, Criado A, Vazquez E, Bianco A, Prato M. Promises, facts and challenges for graphene in biomedical applications. Chem Soc Rev. 2017;46(15):4400–16.

108. Bianco A. Graphene: safe or toxic? The two faces of the medal. Angew Chem Int Ed Engl. 2013;52(19):4986–97.
109. Wick P, Louw-Gaume AE, Kucki M, Krug HF, Kostarelos K, Fadeel B, et al. Classification framework for graphene-based materials. Angew Chem Int Ed Engl. 2014;53(30):7714–8.
110. Ou L, Song B, Liang H, Liu J, Feng X, Deng B, et al. Toxicity of graphene-family nanoparticles: a general review of the origins and mechanisms. Part Fibre Toxicol. 2016;13:57.
111. Kenry LCT. Biocompatibility and nanotoxicity of layered two-dimensional nanomaterials. ChemNanoMat. 2017;3(1):5–16.
112. Mukherjee SP, Lozano N, Kucki M, Del Rio-Castillo AE, Newman L, Vazquez E, et al. Detection of endotoxin contamination of graphene based materials using the TNF-α expression test and guidelines for endotoxin-free graphene oxide production. PLoS One. 2016;11:e0166816.
113. Vranic S, Rodrigues AF, Buggio M, Newman L, White MRH, Spiller DG, et al. Live imaging of label-free graphene oxide reveals critical factors causing oxidative-stress-mediated cellular responses. ACS Nano. 2018;12(2):1373–89.
114. Castagnola V, Zhao W, Boselli L, Lo Giudice MC, Meder F, Polo E, et al. Biological recognition of graphene nanoflakes. Nat Commun. 2018;9:1577.
115. Shin SR, Li YC, Jang HL, Khoshakhlagh P, Akbari M, Nasajpour A, et al. Graphene-based materials for tissue engineering. Adv Drug Deliv Rev. 2016;105(PartB):255–74.
116. Vale FM, Castro M, Monteiro J, Couto FS, Pinto R, Rico JMGT. Acrylic bone cement induces the production of free radicals by cultured human fibroblasts. Biomaterials. 1997;18(16):1133–5.
117. Yang SY, Oh JG, Jung DY, Choi HK, Yu CH, Shin J, et al. Metal-etching-free direct delamination and transfer of single-layer graphene with a high degree of freedom. Small. 2015;11:175–81.
118. Hussain SM, Frazier JM. Cellular toxicity of hydrazine in primary rat hepatocytes. Toxicol Sci. 2002;69(2):424–32.
119. Zhang J, Yang H, Shen G, Cheng P, Zhang J, Guo S. Reduction of graphene oxide via L-ascorbic acid. Chem Commun. 2010;46(7):1112–4.
120. Evariste L, Lagier L, Gonzalez P, Mottier A, Mouchet F, Cadarsi S, et al. Thermal reduction of graphene oxide mitigates its *in vivo* genotoxicity toward xenopus laevis tadpoles. Nanomaterials. 2019;9(4):584.
121. Toh SY, Loh KS, Kamarudin SK, Daud WRW. Graphene production via electrochemical reduction of graphene oxide: synthesis and characterisation. Chem Eng J. 2014;251:422–34.
122. Lisi N, Dikonimos T, Buonocore F, Pittori M, Mazzaro R, Rizzoli R, et al. Contamination-free graphene by chemical vapor deposition in quartz furnaces. Sci Rep. 2017;7:9927.
123. González VJ, Rodríguez AM, León V, Frontiñán-Rubio J, Fierro JLG, Durán-Prado M, et al. Sweet graphene: exfoliation of graphite and preparation of glucose-graphene cocrystals through mechanochemical treatments. Green Chem. 2018;20(15):3581–92.
124. Chatterjee N, Eom HJ, Choi J. A systems toxicology approach to the surface functionality control of graphene-cell interactions. Biomaterials. 2014;35(4):1109–27.
125. Masvidal-Codina E, Illa X, Dasilva M, Calia AB, Dragojević T, Vidal-Rosas EE, et al. High-resolution mapping of infraslow cortical brain activity enabled by graphene microtransistors. Nat Mater. 2019;18(3):280–8.
126. Drasler B, Kucki M, Delhaes F, Buerki-Thurnherr T, Vanhecke D, Korejwo D, et al. Single exposure to aerosolized graphene oxide and graphene nanoplatelets did not initiate an acute biological response in a 3D human lung model. Carbon. 2018;137:125–35.
127. Guarnieri D, Sánchez-Moreno P, Del Rio Castillo AE, Bonaccorso F, Gatto F, Bardi G, et al. Biotransformation and biological interaction of graphene and graphene oxide during simulated oral ingestion. Small. 2018;14(24):e1800227.
128. Sasidharan A, Panchakarla LS, Sadanandan AR, Ashokan A, Chandran P, Girish CM, et al. Hemocompatibility and macrophage response of pristine and functionalized graphene. Small. 2012;8(8):1251–63.
129. Liu JH, Yang ST, Wang H, Chang Y, Cao A, Liu Y. Effect of size and dose on the biodistribution of graphene oxide in mice. Nanomed. 2012;7(12):1801–12.
130. Zhang X, Wei C, Li Y, Li Y, Chen G, He Y, et al. Dose-dependent cytotoxicity induced by pristine graphene oxide nanosheets for potential bone tissue regeneration. J Biomed Mater Res A. 2020;108(3):614–24.
131. Cheng C, Nie S, Li S, Peng H, Yang H, Ma L, et al. Biopolymer functionalized reduced graphene oxide with enhanced biocompatibility via mussel inspired coatings/anchors. J Mater Chem B. 2013;1(3):265–75.
132. Pinto AM, Moreira JA, Magalhães FD. Gonçalves IC; Polymer surface adsorption as a strategy to improve the biocompatibility of graphene nanoplatelets. Colloids Surf B Biointerfaces. 2016;146:818–24.
133. Sasidharan A, Swaroop S, Koduri CK, Girish CM, Chandran P, Panchakarla LS, et al. Comparative *in vivo* toxicity, organ biodistribution and immune response of pristine, carboxylated and PEGylated few-layer graphene sheets in Swiss albino mice: a three month study. Carbon. 2015;95:511–24.
134. Jasim DA, Murphy S, Newman L, Mironov A, Prestat E, McCaffrey J, et al. The effects of extensive glomerular filtration of thin graphene oxide sheets on kidney physiology. ACS Nano. 2016;10(12):10753–67.
135. Xu M, Zhu J, Wang F, Xiong Y, Wu Y, Wang Q, et al. Improved *in vitro* and *in vivo* biocompatibility of graphene oxide through surface modification: poly(acrylic acid)-functionalization is superior to PEGylation. ACS Nano. 2016;10(3):3267–81.
136. Russier J, Treossi E, Scarsi A, Perrozzi F, Dumortier H, Ottaviano L, et al. Evidencing the mask effect of graphene oxide: a comparative study on primary human and murine phagocytic cells. Nanoscale. 2013;5(22):11234–47.
137. Yue H, Wei W, Yue Z, Wang B, Luo N, Gao Y, et al. The role of the lateral dimension of graphene oxide in the regulation of cellular responses. Biomaterials. 2012;33(16):4013–21.
138. Cicuéndez M, Fernandes M, Ayán-Varela M, Oliveira H, Feito MJ, Diez-Orejas R, et al. Macrophage inflammatory and metabolic responses to graphene-based nanomaterials differing in size and functionalization. Colloids Surf B Biointerfaces. 2020;186:110709.
139. Mukherjee SP, Kostarelos K, Fadeel B. Cytokine profiling of primary human macrophages exposed to endotoxin-free graphene oxide: size-independent NLRP3 inflammasome activation. Adv Healthc Mater. 2018;7(4):1700815.
140. Svadlakova T, Hubatka F, Knotigova PT, Kulich P, Masek J, Kotoucek J, et al. Proinflammatory effect of carbon-based nanomaterials: *in vitro* study on stimulation of inflammasome NLRP3 via destabilisation of lysosomes. Nanomaterials. 2020;10(3):418.
141. Luo N, Ni D, Yue H, Wei W, Ma G. Surface-engineered graphene navigate divergent biological outcomes toward macrophages. ACS Appl Mater Interfaces. 2015;7(9):5239–47.
142. Luo N, Weber JK, Wang S, Luan B, Yue H, Xi X, et al. PEGylated graphene oxide elicits strong immunological responses despite surface passivation. Nat Commun. 2017;8:14537.
143. Mukherjee SP, Lazzaretto B, Hultenby K, Newman L, Rodrigues AF, Lozano N, et al. Graphene oxide elicits membrane lipid changes and neutrophil extracellular trap formation. Chemistry. 2018;4(2):334–58.
144. Liao KH, Lin YS, MacOsko CW, Haynes CL. Cytotoxicity of graphene oxide and graphene in human erythrocytes and skin fibroblasts. ACS Appl Mater Interfaces. 2011;3(7):2607–15.

145. Pelin M, Fusco L, Martín C, Sosa S, Frontiñán-Rubio J, González-Domínguez JM, et al. Graphene and graphene oxide induce ROS production in human HaCaT skin keratinocytes: the role of xanthine oxidase and NADH dehydrogenase. Nanoscale. 2018;10(25):11820–30.
146. Fusco L, Pelin M, Mukherjee S, Keshavan S, Sosa S, Martín C, et al. Keratinocytes are capable of selectively sensing low amounts of graphene-based materials: implications for cutaneous applications. Carbon. 2020;159:598–610.
147. Erf GF, Falcon DM, Sullivan KS, Bourdo SE. T lymphocytes dominate local leukocyte infiltration in response to intradermal injection of functionalized graphene-based nanomaterial. J Appl Toxicol. 2017;37(11):1317–24.
148. Bramini M, Alberini G, Colombo E, Chiacchiaretta M, DiFrancesco ML, Maya-Vetencourt JF, et al. Interfacing graphene-based materials with neural cells. Front Syst Neurosci. 2018;12:12.
149. Bramini M, Sacchetti S, Armirotti A, Rocchi A, Vázquez E, León Castellanos V, et al. Graphene oxide nanosheets disrupt lipid composition, Ca^{2+} homeostasis, and synaptic transmission in primary cortical neurons. ACS Nano. 2016;10(7):7154–71.
150. Rauti R, Medelin M, Newman L, Vranic S, Reina G, Bianco A, et al. Graphene oxide flakes tune excitatory neurotransmission *in vivo* by targeting hippocampal synapses. Nano Lett. 2019;19(5):2858–70.
151. Chiacchiaretta M, Bramini M, Rocchi A, Armirotti A, Giordano E, Vázquez E, et al. Graphene oxide upregulates the homeostatic functions of primary astrocytes and modulates astrocyte-to-neuron communication. Nano Lett. 2018;18(9):5827–38.
152. Bramini M, Chiacchiaretta M, Armirotti A, Rocchi A, Kale DD, Martin C, et al. An increase in membrane cholesterol by graphene oxide disrupts calcium homeostasis in primary astrocytes. Small. 2019;15(15):1900147.
153. Durso M, Borrachero-Conejo AI, Bettini C, Treossi E, Scidà A, Saracino E, et al. Biomimetic graphene for enhanced interaction with the external membrane of astrocytes. J Mater Chem B. 2018;6(33):5335–42.
154. Kitko KE, Hong T, Lazarenko RM, Ying D, Xu YQ, Zhang Q. Membrane cholesterol mediates the cellular effects of monolayer graphene substrates. Nat Commun. 2018;9:796.
155. Chen X, Park YJ, Kang M, Kang SK, Koo J, Shinde SM, et al. CVD-grown monolayer MoS_2 in bioabsorbable electronics and biosensors. Nat Commun. 2018;9:1690.
156. Mendonca MC, Soares ES, de Jesus MB, Ceragioli HJ, Irazusta SP, Batista AG, et al. Reduced graphene oxide: nanotoxicological profile in rats. J Nanobiotechnol. 2016;14:53.
157. Mendonca MC, Soares ES, de Jesus MB, Ceragioli HJ, Batista AG, Nyul-Toth A, et al. PEGylation of reduced graphene oxide induces toxicity in cells of the blood-brain barrier: an *in vitro* and *in vivo* study. Mol Pharm. 2016;13(11):3913–24.
158. Pampaloni NP, Lottner M, Giugliano M, Matruglio A, D'Amico F, Prato M, et al. Single-layer graphene modulates neuronal communication and augments membrane ion currents. Nat Nanotechnol. 2018;13:755–64.
159. Park SY, Park J, Sim SH, Sung MG, Kim KS, Hong BH, et al. Enhanced differentiation of human neural stem cells into neurons on graphene. Adv Mater. 2011;23(36):H263–7.
160. Liao C, Li Y, Tjong SC. Graphene nanomaterials: synthesis, biocompatibility, and cytotoxicity. Int J Mol Sci. 2018;19(11):3564.
161. Bae S, Kim H, Lee Y, Xu X, Park JS, Zheng Y, et al. Roll-to-roll production of 30-inch graphene films for transparent electrodes. Nat Nanotechnol. 2010;5:574–8.
162. Park J, Park S, Ryu S, Bhang SH, Kim J, Yoon JK, et al. Graphene-regulated cardiomyogenic differentiation process of mesenchymal stem cells by enhancing the expression of extracellular matrix proteins and cell signaling molecules. Adv Healthc Mater. 2014;3(2):176–81.
163. Ali-Boucetta H, Bitounis D, Raveendran-Nair R, Servant A, Van den Bossche J, Kostarelos K. Purified graphene oxide dispersions lack *in vitro* cytotoxicity and *in vivo* pathogenicity. Adv Healthc Mater. 2013;2(3):433–41.
164. Zhang Y, Nayak TR, Hong H, Cai W. Graphene: a versatile nanoplatform for biomedical applications. Nanoscale. 2012;4(13):3833–42.
165. Zhang Y, Ali SF, Dervishi E, Xu Y, Li Z, Casciano D, et al. Cytotoxicity effects of graphene and single-wall carbon nanotubes in neural phaeochromocytoma-derived PC12 cells. ACS Nano. 2010;4(6):3181–6.
166. Schinwald A, Murphy FA, Jones A, Macnee W, Donaldson K. Graphene-based nanoplatelets: a new risk to the respiratory system. ACS Nano. 2012;6(1):736–46.
167. Teo WZ, Chng ELK, Sofer Z, Pumera M. Cytotoxicity of exfoliated transition-metal dichalcogenides (MoS_2, WS_2, and WSe_2) is lower than that of graphene and its analogues. Chem Eur J. 2014;20(31):9627–32.
168. Dhenadhayalan N, Yadav K, Sriram MI, Lee HL, Lin KC. Ultrasensitive DNA sensing of a prostate-specific antigen based on 2D nanosheets in live cells. Nanoscale. 2017;9(33):12087–95.
169. Ayán-Varela M, Pérez-Vidal Ó, Paredes JI, Munuera JM, Villar-Rodil S, Díaz-González M, et al. Aqueous exfoliation of transition metal dichalcogenides assisted by DNA/RNA nucleotides: catalytically active and biocompatible nanosheets stabilized by acid-base interactions. ACS Appl Mater Interfaces. 2017;9(3):2835–45.
170. Guan G, Zhang S, Liu S, Cai Y, Low M, Teng CP, et al. Protein induces layer-by-layer exfoliation of transition metal dichalcogenides. J Am Chem Soc. 2015;137(19):6152–5.
171. Wang X, Mansukhani ND, Guiney LM, Ji Z, Chang CH, Wang M, et al. Differences in the toxicological potential of 2D versus aggregated molybdenum disulfide in the lung. Small. 2015;11(38):5079–87.
172. Chng ELK, Sofer Z, Pumera M. MoS_2 exhibits stronger toxicity with increased exfoliation. Nanoscale. 2014;6(23):14412–8.
173. Liu T, Shi S, Liang C, Shen S, Cheng L, Wang C, et al. Iron oxide decorated MoS_2 nanosheets with double PEGylation for chelator-free radiolabeling and multimodal imaging guided photothermal therapy. ACS Nano. 2015;9(1):950–60.
174. Kim J, Kim H, Kim WJ. Single-layered MoS_2-PEI-PEG nanocomposite-mediated gene delivery controlled by photo and redox stimuli. Small. 2016;12(9):1184–92.
175. Liu T, Wang C, Gu X, Gong H, Cheng L, Shi X, et al. Drug delivery with PEGylated MoS_2 nano-sheets for combined photothermal and chemotherapy of cancer. Adv Mater. 2014;26(21):3433–40.
176. Kaur J, Singh M, Dell'Aversana C, Benedetti R, Giardina P, Rossi M, et al. Biological interactions of biocompatible and water-dispersed MoS_2 nanosheets with bacteria and human cells. Sci Rep. 2018;8:16386.
177. Shah P, Narayanan TN, Li CZ, Alwarappan S. Probing the biocompatibility of MoS_2 nanosheets by cytotoxicity assay and electrical impedance spectroscopy. Nanotechnology. 2015;26(31):315102.
178. Appel JH, Li DO, Podlevsky JD, Debnath A, Green AA, Wang QH, et al. Low cytotoxicity and genotoxicity of two-dimensional MoS_2 and WS_2. ACS Biomater Sci Eng. 2016;2(3):361–7.
179. Kim JE, Yim D, Han SW, Nam J, Kim JH, Kim JW. Effective suppression of oxidative stress on living cells in hydrogel particles containing a physically immobilized WS_2 radical scavenger. ACS Appl Mater Interfaces. 2019;11(20):18817–24.

180. Szuplewska A, Wojciechowski T, Chudy M, Ziemkowska W, Chlubny L, Olszyna A. *In vitro* studies on cytotoxicity of delaminated Ti_3C_2 MXene. J Hazard Mater. 2017;339:1–8.
181. Liang R, Li Y, Huo M, Lin H, Chen Y. Triggering sequential catalytic Fenton reaction on 2D MXenes for hyperthermia-augmented synergistic nanocatalytic cancer therapy. ACS Appl Mater Interfaces. 2019;11(46):42917–31.
182. Rafieerad A, Sequiera GL, Yan W, Kaur P, Amiri A, Dhingra S. Sweet-MXene hydrogel with mixed-dimensional components for biomedical applications. J Mech Behav Biomed Mater. 2020;101:103440.
183. Driscoll N, Richardson AG, Maleski K, Anasori B, Adewole O, Lelyukh P, et al. Two-dimensional Ti_3C_2 MXene for high- resolution neural interfaces. ACS Nano. 2018;12(10):10419–29.
184. Zhang J, Fu Y, Mo A. Multilayered titanium carbide MXene film for guided bone regeneration. Int J Nanomedicine. 2019;14:10091–103.
185. Kurapati R, Backes C, Menard-Moyon C, Coleman JN, Bianco A. White graphene undergoes peroxidase degradation. Angew Chem Int Ed Engl. 2016;55(18):5506–11.
186. Mukherjee SP, Gliga AR, Lazzaretto B, Brandner B, Fielden M, Vogt C, et al. Graphene oxide is degraded by neutrophils and the degradation products are non-genotoxic. Nanoscale. 2018;10:1180–8.
187. Kurapati R, Mukherjee SP, Martín C, Bepete G, Vázquez E, Pénicaud A, et al. Degradation of single-layer and few-layer graphene by neutrophil myeloperoxidase. Angew Chem Int Ed. 2018;57(6):11722–7.
188. Newman L, Lozano N, Zhang M, Iijima S, Yudasaka M, Bussy C, et al. Hypochlorite degrades 2D graphene oxide sheets faster than 1D oxidised carbon nanotubes and nanohorns. npj 2D. Mater Appl. 2017;1:39.
189. Li Y, Feng L, Shi X, Wang X, Yang Y, Yang K, et al. Surface coating-dependent cytotoxicity and degradation of graphene derivatives: towards the design of non-toxic, degradable nano-graphene. Small. 2014;10(8):1544–54.
190. Kurapati R, Bonachera F, Russier J, Sureshbabu AR, Ménard-Moyon C, Kostarelos K, et al. Covalent chemical functionalization enhances the biodegradation of graphene oxide. 2D Mater. 2018;5(1):015020.
191. Mei L, Zhang X, Yin W, Dong X, Guo Z, Fu W, et al. Translocation, biotransformation-related degradation, and toxicity assessment of polyvinylpyrrolidone-modified 2H-phase nano-MoS_2. Nanoscale. 2019;11:4767–80.